sciendo
Power Electronics and Drives
Volume 8(43), 2023 DOI: 10.2478/pead-2023-0022
Power Electronics and Drives

Nonlinear Optimal Control for the Nine-Phase Permanent Magnet Synchronous Motor

Research paper

Gerasimos G. Rigatos[1,*], Pierluigi Siano[2], Mohammed AL Numay[3], Masoud Abbaszadeh[4], Bilal Sari[5], Khmaies Ouahada[6]

[1]*Industrial Systems Institute, Unit of Industrial Automation Industrial Systems Institute, Rion Patras, Greece*
[2]*Department of Management and Innovation Systems, University of Salerno, Italy*
[3]*Department of Electrical Engineering, King Saud University, Saudi Arabia*
[4]*Department of ECS Engineering, Rensselaer Polytechnic Institute, USA*
[5]*Department of Electrical Engineering, University of Setif I, Algeria*
[6]*Department of Electrical and Electronic Engineering Science, University of Johanessburg, South Africa*

Received: 11 June, 2023; Accepted: 05 September, 2023

Abstract: Multi-phase electric motors and in particular nine-phase permanent magnet synchronous motors (9-phase PMSMs) find use in electric actuation, traction and propulsion systems. They exhibit advantages comparing to three-phase motors because of achieving high power and torque rates under moderate variations of voltage and currents in their phases, while also exhibiting fault tolerance. In this article a novel nonlinear optimal control method is developed for the dynamic model of nine-phase PMSMs. First it is proven that the dynamic model of these motors is differentially flat. Next, to apply the proposed nonlinear optimal control, the state-space model of the nine-phase PMSM undergoes an approximate linearization process at each sampling instance. The linearisation procedure is based on first-order Taylor-series expansion and on the computation of the system's Jacobian matrices. It takes place at each sampling interval around a temporary operating point which is defined by the present value of the system's state vector and by the last sampled value of the control inputs vector. For the linearized model of the system an H-infinity feedback controller is designed. To compute the feedback gains of this controller an algebraic Riccati equation is repetitively solved at each time-step of the control algorithm. The global stability properties of the control scheme are proven through Lyapunov analysis. First it is demonstrated that the H-infinity tracking performance criterion is satisfied, which signifies robustness of the control scheme against model uncertainty and perturbations. Moreover, under mild assumptions it is also proven that the control loop is globally asymptotically stable. Additionally it is experimentally confirmed through simulation tests, that the nonlinear optimal control method achieves fast and accurate tracking of reference setpoints under moderate variations of the control inputs. Finally, to apply state estimation-based control without the need to measure the entire state vector of the nine-phase PMSM, the H-infinity Kalman Filter is used as a robust state estimator.

Keywords: *nine-phase PMSM • differential flatness-properties • nonlinear optimal control • H-infinity control • approximate linearization, Taylor-series expansion • Jacobian matrices • Riccati equation • Lyapunov analysis • global stability*

1. Introduction

Multi-phase electric motors and particularly nine-phase permanent magnet synchronous motors exhibit several advantages in applications of electric traction and propulsion when compared to three-phase synchronous or asynchronous motors (Wang, Wu et al., 2023), (Wang, Wu et al., 2023). This is because they achieve improved power and torque rates while also keeping moderate values for the currents and voltages of their multiple phases (Wang, Zheng et al., 2022), (Prieto-Araujo et al., 2015). By exhibiting redundancy in phases such motors are less prone to a total failure and remain functional under harsh operating conditions (Slunjski et al., 2021), (Rubins et al., 2020).

* *Email: grigat@ieee.org*

Considering the high power and torque that nine-phase PMSMs can generate, the suitability of such motors for the traction of heavy duty electric vehicles can be also concluded (Wang, Xu et al., 2023), (Liu et al., 2020). At the same time these motors have a nonlinear and multivariable dynamic model which requires the application of elaborated nonlinear control methods (Wang, Zhu et al., 2023), (Tong et al., 2023). So far several nonlinear control schemes have been proposed for nine-phase PMSMs (Zhao et al., 2020), (Jung et al., 2012). One can distinguish several model predictive control approaches for these motors (Garcia-Entrambosaguas, 2019), (Cheng, Yu et al., 2016). Stability and robustness issues in these control techniques remain often a research challenge (Wang et al., 2023), (Slunjski et al., 2019). Fault tolerance is a primary objective in the control loop design for nine-phase motors (Mohamadian and Cecati, 2021), (Mohamadian et al., 2023). Furthermore, implementation of sensorless control with the use of state observers or filters is also among the aims of controller design for nine-phase PMSMs (Stiscia et al., 2019), (Wang, Wu and Wang, 2022).

In this article a novel nonlinear optimal control method is proposed for nine-phase PMSMs. First, the dynamic model of these motors is given in state-space form. With the use Clarke's and Park's generalized transformations one moves from the initial description of the motor in three *abc* three-phase reference frames into an equivalent description in three *dq* two-phase frames (Kozovsky, Blaha and Vaclavek, 2016), (Kozovsky and Blaha, 2017). The state vector of the motor has eight state variables out of which the first two are the turn angle and speed of the motor while the rest six are current variables of the *dq* frames of the stator. The motor has a control inputs vector with six variables which are the windings' input voltages expressed in the *dq* frames of the stator (Kozovsky, Blaha and Vaclavek, 2016), (Kozovsky and Blaha, 2017). The model is written in the nonlinear affine-in-the-input state-space form and is proven to be differentially flat (Rigatos, 2015). The differential flatness properties are also an implicit proof of the system's controllability and allow for defining feasible setpoints for all state variables of the motor. To implement the proposed nonlinear optimal control scheme, the dynamic model of the nine-phase PMSM undergoes approximate linearization with the use of first-order Taylor series expansion and through the computation of the associated Jacobian matrices (Rigatos, 2016), (Rigatos, Abbaszadeh and Hamida, 2023), (Rigatos and Karapanou, 2020). The linearization takes place at each sampling instant around a time-varying operating point which is defined by the present value of the system's state vector and the last sampled value of the control inputs vector (Rigatos and Tzafestas, 2007), (Rigatos and Nikiforov, 1993), (Rigatos and Zhang, 2009). For the approximately linearized model of the system a stabilizing H-infinity feedback controller is designed.

The proposed H-infinity controller achieves a solution for the optimal control problem of the 9-phase PMSM under model uncertainty and exogenous perturbations. Actually, it represents a min-max differential game taking place between (i) the control inputs of the system which try to minimize a cost function that contains a quadratic term of the state vector's tracking error, (ii) model uncertainty and exogenous perturbations which try to maximize this cost function. To select the feedback gains of this controller an algebraic Riccati equation is repetitively solved at each time-step of the control algorithm (Rigatos, 2016), (Rigatos, Abbaszadeh and Hamida, 2023), (Rigatos and Karapanou, 2020). The global stability properties of the control scheme are proven through Lyapunov analysis. First, it is proven that the controller satisfies the H-infinity tracking performance criterion. This signifies that the control method is robust to model imprecision and disturbances (Toussaint et al., 2000). Moreover, under moderate conditions it is also proven that the control loop is globally asymptotically stable. To implement state estimation-based control without the need to measure the entire state vector of the 9-phase PMSM, the H-infinity Kalman Filter is used as a robust state estimator. The method achieves fast and accurate tracking of reference setpoints under moderate variations of the control inputs (Rigatos, 2016), (Rigatos, Abbaszadeh and Hamida, 2023), (Rigatos and Karapanou, 2020).

The significance of the article's results and methods is outlined in the following (Rigatos, 2016), (Rigatos, Abbaszadeh and Hamida, 2023), (Rigatos and Karapanou, 2020): (i) The presented nonlinear optimal control method does not use complicated transformations of the state-space model of the controlled system and changes of state variables. The computed control inputs are applied directly on the initial nonlinear state-space model of the system thus avoiding inverse transformations and the associated singularity issues (ii) The use of the nonlinear optimal control method does not have as a prerequisite the system to be found or to be transformed into a specific state-space form, as for instance the canonical (input-output linearized) form, or the triangular (backstepping integral) form (c) the convergence of the method's iterative search for the optimum is not dependent on parameter values selection and ad-hoc initialization (met for instance in NMPC) and its global stability properties are proven through Lyapunov analysis, (iv) the method is computationally efficient and energy efficient. It is computationally efficient because of linearizing around one single operating point and because of solving only one Riccati equation (in place of LMIs). It is energy efficient because of minimizing the variations of the control inputs, thus also reducing the dispersion of energy by the control loop.

The novelty of the article's results and methods is justified in the following (Rigatos, 2016), (Rigatos, Abbaszadeh and Hamida, 2023), (Rigatos and Karapanou, 2020): Unlike past approaches, in the new nonlinear optimal control method linearization is performed around a temporary operating point which is defined by the present value of the system's state vector and by the last sampled value of the control inputs vector and not at points that belong to the desirable trajectory (setpoints). Besides, the Riccati equation which is used for computing the feedback gains of the controller is new, and so is the global stability proof for this control method. Comparing to NMPC (Nonlinear Model Predictive Control) which is a popular approach for treating the optimal control problem in industry, the new nonlinear optimal (H-infinity) control scheme is of proven global stability and the convergence of its iterative search for the optimum does not depend on initial conditions and on trials with multiple sets of controller parameters. It is also noteworthy that the nonlinear optimal control method is applicable to a wider class of dynamical systems than approaches based on the solution of State Dependent Riccati Equations (SDRE). The SDRE approaches can be applied only to dynamical systems which can be transformed to the Linear Parameter Varying (LPV) form. Besides, the nonlinear optimal control method performs better than nonlinear optimal control schemes which use approximation of the solution of the Hamilton-Jacobi-Bellman equation by Galerkin series expansions. The stability properties of the Galerkin series expansion -based optimal control approaches are still unproven.

The structure of the paper is as follows: In Section 2 the dynamic model of the 9-phase PMSM is analyzed and the associated state-space model is formulated. In Section 3 it is proven that the dynamic model of the nine-phase PMSM is a differentially flat system. In Section 4 approximate linearization is performed on the model of the nine-phase PMSM through first-order Taylor series expansion and the computation of the associated Jacobian matrices. In Section 5 an H-infinity feedback controller is designed for the nine-phase PMSM thus providing a solution to this system's nonlinear optimal control problem, In Section 6 the global stability properties of the nonlinear optimal (H-infinity) control method are proven through Lyapunov analysis. In Section 7 the fine performance of the nonlinear optimal control method is tested through simulation experiments. Finally, in Section 8 concluding remarks are stated.

2. Dynamic model of the nine-phase PMSM

Nine-phase permanent magnet synchronous motors are used in electric actuation, traction and propulsion systems where high power and torque is needed. Therefore, they are a promising solution for electric traction of heavy duty vehicles. The diagram of the triple three-phase frames for the 9-phase permanent magnet synchronous motor is shown in Fig. 1 (Kozovsky, Blaha and Vaclavek, 2016), (Kozovsky and Blaha, 2017).

Initially, a triple three-phase notation is considered for the motor's voltages and currents, which is denoted as $(a_1, b_1, c_1),\ (a_2, b_2, c_2)$, and (a_3, b_3, c_3). After applying Clarke's and Park's generalized transformations the three-phase ***abc*** frames are turned into two-phase ***dq*** frames which are synchronously rotating with the motor and which are denoted as $(d_1, q_1),\ (d_2, q_2)$ and (d_3, q_3) (Kozovsky, Blaha and Vaclavek, 2016), (Kozovsky and Blaha, 2017).

The application of Kirchhoff's voltage laws in each one these ***dq*** frames $j = 1, 2, 3$ gives the set of equations:

$$\begin{aligned} v_{d1} &= R_1 i_{d1} + \tfrac{d\psi_{d1}}{dt} - \omega\psi_{d1} \\ v_{q1} &= R_1 i_{q1} + \tfrac{d\psi_{q1}}{dt} + \omega\psi_{q1} \end{aligned} \tag{1}$$

$$\begin{aligned} v_{d2} &= R_2 i_{d2} + \tfrac{d\psi_{d2}}{dt} - \omega\psi_{d2} \\ v_{q2} &= R_2 i_{q2} + \tfrac{d\psi_{q2}}{dt} + \omega\psi_{q2} \end{aligned} \tag{2}$$

$$\begin{aligned} v_{d3} &= R_3 i_{d3} + \tfrac{d\psi_{d3}}{dt} - \omega\psi_{d3} \\ v_{q3} &= R_3 i_{q3} + \tfrac{d\psi_{q3}}{dt} + \omega\psi_{q3} \end{aligned} \tag{3}$$

$v_{d,j},\ v_{q,j}$ are voltage variables on the d and q axis, $i_{d,j},\ i_{q,j}$ are current variables on the d and q axis, and $\psi_{d,j},\ \psi_{q,j}$ are magnetic flux variables on the d and q axis.

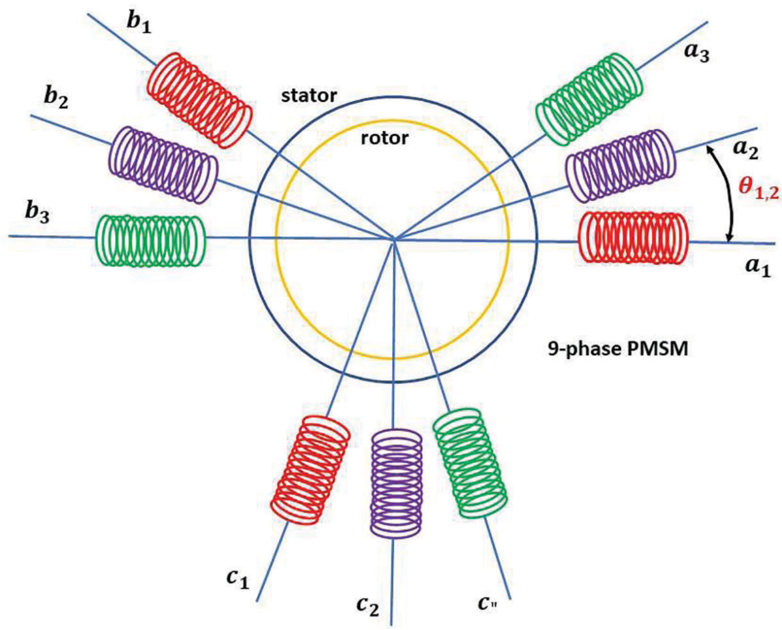

Fig. 1. Diagram of the triple three-phase frames for the 9-phase permanent magnet synchronous motor.

Moreover, the equations describing the variations of the magnetic flux of the rotor $\psi_{d,j},\ \psi_{q,j},\ j=1,2,3$ take into account the effects of the mutual inductance between the phases as shown in the following equations: (Kozovsky, Blaha and Vaclavek, 2016), (Kozovsky and Blaha, 2017)

$$\begin{aligned}\psi_{d1} &= \Psi_{M,d1} + L_{d1}i_{d1} + M_{d1,d2}i_{d2} + M_{d1,d3}i_{d3} \\ \psi_{q1} &= L_{q1}i_{q1} + M_{q1,q2}i_{q2} + M_{q1,q3}i_{q3}\end{aligned} \tag{4}$$

$$\begin{aligned}\psi_{d2} &= \Psi_{M,d2} + L_{d2}i_{d2} + M_{d1,d2}i_{d1} + M_{d2,d3}i_{d3} \\ \psi_{q2} &= L_{q2}i_{q2} + M_{q1,q2}i_{q1} + M_{q1,q3}i_{q3}\end{aligned} \tag{5}$$

$$\begin{aligned}\psi_{d3} &= \Psi_{M,d3} + L_{d3}i_{d3} + M_{d1,d3}i_{d1} + M_{d2,d3}i_{d2} \\ \psi_{q3} &= L_{q3}i_{q3} + M_{q1,q3}i_{q1} + M_{q2,q3}i_{q2}\end{aligned} \tag{6}$$

Next, it is considered that all inductance coefficients of the d-axis and q-axis take the same values L_d and L_q respectively. Moreover, it is considered that all mutual inductance coefficients of the d-axis and q-axis take the same value M_d and M_q respectively.

Using Eq. (1) to Eq. (3) jointly with Eq. (4) to Eq. (6) the electric dynamics of the nine-phase PMSM is described by the following set of equations (Kozovsky, Blaha and Vaclavek, 2016), (Kozovsky and Blaha, 2017):

$$v_{d1} = L_d\frac{di_{d1}}{dt} + M_d\frac{di_{d2}}{dt} + M_d\frac{di_{d3}}{dt} + Ri_{d1} - \omega(L_qi_{q1} + M_di_{q2} + M_qi_{q3}) \tag{7}$$

$$v_{d2} = M_d\frac{di_{d1}}{dt} + L_d\frac{di_{d2}}{dt} + M_d\frac{di_{d3}}{dt} + Ri_{d2} - \omega(M_qi_{q1} + L_qi_{q2} + M_qi_{q3}) \tag{8}$$

$$v_{d3} = M_d\frac{di_{d1}}{dt} + M_d\frac{di_{d2}}{dt} + L_d\frac{di_{d3}}{dt} + Ri_{d3} - \omega(M_qi_{q1} + M_qi_{q2} + L_qi_{q3}) \tag{9}$$

$$v_{q1} = \omega(L_di_{d1} + M_di_{d2} + M_di_{d3} + \Psi_M) + L_q\frac{di_{q1}}{dt} + M_q\frac{di_{q2}}{dt} + M_q\frac{di_{q3}}{dt} + Ri_{q1} \tag{10}$$

$$v_{q2} = \omega(M_di_{d1} + L_di_{q2} + M_di_{d3} + \Psi_M) + M_q\frac{di_{q1}}{dt} + L_q\frac{di_{q2}}{dt} + M_q\frac{di_{q3}}{dt} + Ri_{q2} \tag{11}$$

$$v_{q3} = \omega(M_di_{d1} + M_di_{q2} + L_di_{d3} + \Psi_M) + M_q\frac{di_{q1}}{dt} + M_q\frac{di_{q2}}{dt} + L_q\frac{di_{q3}}{dt} + Ri_{q3} \tag{12}$$

The state variables for the model of the electric dynamics of the 9-phase PMSM constitute the currents vector $[i_{d1}, i_{q1}, i_{d2}, i_{q2}, i_{d3}, i_{q3}]^T$.

The control variables for the model of the electric dynamics of the 9-phase PMSM constitute the control inputs vector $[v_{d1}, v_{q1}, v_{d2}, v_{q2}, v_{d3}, v_{q3}]^T$. Thus, one obtains the following matrix description about the electric dynamics of the 9-phase PMSM

$$
\begin{pmatrix} L_d & 0 & M_d & 0 & M_d & 0 \\ 0 & L_q & 0 & M_q & 0 & M_q \\ M_d & 0 & L_d & 0 & M_d & 0 \\ 0 & M_q & 0 & L_q & 0 & M_q \\ M_d & 0 & M_d & 0 & L_d & 0 \\ 0 & M_q & 0 & M_q & 0 & M_q \end{pmatrix} \begin{pmatrix} \frac{di_{d1}}{dt} \\ \frac{di_{q1}}{dt} \\ \frac{di_{d2}}{dt} \\ \frac{di_{q2}}{dt} \\ \frac{di_{d3}}{dt} \\ \frac{di_{q3}}{dt} \end{pmatrix} +
$$

$$
+ \begin{pmatrix} R & -\omega L_q & 0 & -\omega M_q & 0 & -\omega M_q \\ \omega L_q & 0 & \omega M_d & 0 & \omega M_d & 0 \\ 0 & -\omega M_q & R & -\omega L_q & 0 & -\omega M_q \\ \omega M_d & 0 & \omega L_d & R & \omega M_d & 0 \\ 0 & -\omega M_q & 0 & -\omega M_q & R & -\omega L_q \\ \omega M_d & 0 & \omega M_d & \omega L_d & R & 0 \end{pmatrix} \begin{pmatrix} i_{d1} \\ i_{q1} \\ i_{d2} \\ i_{q2} \\ i_{d3} \\ i_{q3} \end{pmatrix} = \begin{pmatrix} v_{d1} \\ v_{q1} \\ v_{d2} \\ v_{q2} \\ v_{d3} \\ v_{q3} \end{pmatrix} \tag{13}
$$

By defining matrix *M* as

$$
M = \begin{pmatrix} L_d & 0 & M_d & 0 & M_d & 0 \\ 0 & L_q & 0 & M_q & 0 & M_q \\ M_d & 0 & L_d & 0 & M_d & 0 \\ 0 & M_q & 0 & L_q & 0 & M_q \\ M_d & 0 & M_d & 0 & L_d & 0 \\ 0 & M_q & 0 & M_q & 0 & M_q \end{pmatrix} \tag{14}
$$

its inverse is found to be

$$
M^{-1} = \begin{pmatrix} \frac{M_{11}}{detM} & -\frac{M_{21}}{detM} & \frac{M_{31}}{detM} & -\frac{M_{41}}{detM} & \frac{M_{51}}{detM} & -\frac{M_{61}}{detM} \\ -\frac{M_{12}}{detM} & \frac{M_{22}}{detM} & -\frac{M_{32}}{detM} & \frac{M_{42}}{detM} & -\frac{M_{52}}{detM} & \frac{M_{62}}{detM} \\ \frac{M_{13}}{detM} & -\frac{M_{23}}{detM} & \frac{M_{33}}{detM} & -\frac{M_{43}}{detM} & \frac{M_{53}}{detM} & -\frac{M_{63}}{detM} \\ -\frac{M_{14}}{detM} & \frac{M_{24}}{detM} & -\frac{M_{34}}{detM} & \frac{M_{44}}{detM} & -\frac{M_{54}}{detM} & \frac{M_{64}}{detM} \\ \frac{M_{15}}{detM} & -\frac{M_{25}}{detM} & \frac{M_{35}}{detM} & -\frac{M_{45}}{detM} & \frac{M_{55}}{detM} & -\frac{M_{65}}{detM} \\ -\frac{M_{16}}{detM} & \frac{M_{26}}{detM} & -\frac{M_{36}}{detM} & \frac{M_{46}}{detM} & -\frac{M_{56}}{detM} & \frac{M_{66}}{detM} \end{pmatrix} \tag{15}
$$

where about the elements of the inverse of matrix M it holds that: $\frac{M_{11}}{detM} = \frac{L_d+M_d}{L_d^2+L_dM_d-2M_d^2}$, $-\frac{M_{21}}{detM} = 0$, $\frac{M_{31}}{detM} = \frac{-M_d}{L_d^2+L_dM_d-2M_d^2}$, $-\frac{M_{41}}{detM} = 0$, $\frac{M_{51}}{detM} = \frac{-M_d}{L_d^2+L_dM_d-2M_d^2}$, $-\frac{M_{61}}{detM} = 0$,
$-\frac{M_{12}}{detM} = 0$, $\frac{M_{22}}{detM} = \frac{L_q+M_q}{L_q^2+L_qM_q-2M_q^2}$, $-\frac{M_{32}}{detM} = 0$, $\frac{M_{42}}{detM} = \frac{-M_q}{L_q^2+L_qM_q-2M_q^2}$, $-\frac{M_{52}}{detM} = 0$, $\frac{M_{62}}{detM} = \frac{-(M_q)}{L_q^2+L_qM_q-2M_q^2}$.
$\frac{M_{13}}{detM} = \frac{-M_d}{L_d^2+L_dM_d-2M_d^2}$, $-\frac{M_{23}}{detM} = 0$, $\frac{M_{33}}{detM} = \frac{L_d+M_d}{L_d^2+L_dM_d-2M_d^2}$, $-\frac{M_{34}}{detM} = 0$, $\frac{M_{35}}{detM} = \frac{-M_d}{L_d^2+L_dM_d-2M_d^2}$, $-\frac{M_{36}}{detM} = 0$.
$-\frac{M_{14}}{detM} = 0$, $\frac{M_{24}}{detM} = \frac{-M_q}{L_q^2+L_qM_q-2M_q^2}$, $-\frac{M_{34}}{detM} = 0$, $\frac{M_{44}}{detM} = \frac{L_q+M_q}{L_q^2+L_qM_q-2M_q^2}$, $-\frac{M_{54}}{detM} = 0$, $\frac{M_{64}}{detM} = \frac{-M_q}{L_q^2+L_qM_q-2M_q^2}$.
$\frac{M_{15}}{detM} = \frac{-M_d}{L_d^2+L_dM_d-2M_d^2}$, $-\frac{M_{25}}{detM} = 0$, $\frac{M_{35}}{detM} = \frac{-M_d}{L_d^2+L_dM_d-2M_d^2}$, $-\frac{M_{45}}{detM} = 0$, $\frac{M_{55}}{detM} = \frac{L_d+M_d}{L_d^2+L_dM_d-2M_d^2}$, $-\frac{M_{65}}{detM} = 0$.
$-\frac{M_{16}}{detM} = 0$, $\frac{M_{26}}{detM} = \frac{-M_q}{L_q^2+L_qM_q-2M_q^2}$, $-\frac{M_{36}}{detM} = 0$, $\frac{M_{46}}{detM} = \frac{-M_q}{L_q^2+L_qM_q-2M_q^2}$, $-\frac{M_{56}}{detM} = 0$, $\frac{M_{66}}{detM} = \frac{L_q+M_q}{L_q^2+L_qM_q-2M_q^2}$.

Moreover, by denoting matrix N as

$$N = \begin{pmatrix} R & -\omega L_q & 0 & -\omega M_q & 0 & -\omega M_q \\ \omega L_q & 0 & \omega M_d & 0 & \omega M_d & 0 \\ 0 & -\omega M_q & R & -\omega L_q & 0 & -\omega M_q \\ \omega M_d & 0 & \omega L_d & R & \omega M_d & 0 \\ 0 & -\omega M_q & 0 & -\omega M_q & R & -\omega L_q \\ \omega M_d & 0 & \omega M_d & \omega L_d & R & 0 \end{pmatrix} \quad (16)$$

the product between matrix M^{-1} and N is $F = M^{-1} \cdot N$

$$F = \begin{pmatrix} F_{11} & F_{12} & F_{13} & F_{14} & F_{15} & F_{16} \\ F_{21} & F_{22} & F_{23} & F_{24} & F_{25} & F_{26} \\ F_{31} & F_{32} & F_{33} & F_{34} & F_{35} & F_{36} \\ F_{41} & F_{42} & F_{43} & F_{44} & F_{45} & F_{46} \\ F_{51} & F_{52} & F_{53} & F_{54} & F_{55} & F_{56} \\ F_{61} & F_{62} & F_{63} & F_{64} & F_{65} & F_{66} \end{pmatrix} \quad (17)$$

where the elements of the product matrix $M \cdot N$ are given by $F_{11} = \frac{M_{11}}{detM}R,\ F_{12} = \frac{M_{11}}{detM}(-\omega L_q) + \frac{M_{31}}{detM}(-\omega M_q) + \frac{M_{51}}{detM}(-\omega M_q),\ F_{13} = \frac{M_{31}}{detM}R,\ F_{14} = \frac{M_{11}}{detM}(-\omega M_q) + \frac{M_{31}}{detM}(-\omega L_q) + \frac{M_{51}}{detM}(-\omega M_q),\ F_{15} = \frac{M_{51}}{detM}R,\ F_{16} = \frac{M_{11}}{detM}(-\omega M_q) + \frac{M_{31}}{detM}(-\omega M_q) + \frac{M_{51}}{detM}(-\omega L_q).$

$F_{21} = \frac{M_{22}}{detM}(\omega L_d) + \frac{M_{42}}{detM}(\omega M_d) + \frac{M_{62}}{detM}(\omega M_d),\ F_{22} = 0,\ F_{23} = \frac{M_{22}}{detM}(\omega M_d) + \frac{M_{42}}{detM}(\omega L_d) + \frac{M_{62}}{detM}(\omega M_d),$ $F_{24} = 0,\ F_{25} = \frac{M_{22}}{detM}(\omega M_d) + \frac{M_{42}}{detM}(\omega M_d) + \frac{M_{62}}{detM}(\omega L_d),\ F_{26} = 0.$

$F_{31} = \frac{M_{13}}{detM}R,\ F_{32} = \frac{M_{13}}{detM}(-\omega L_q) + \frac{M_{33}}{detM}(-\omega M_q) + \frac{M_{53}}{detM}(-\omega M_q),\ F_{33} = \frac{M_{33}}{detM}R,\ F_{34} = \frac{M_{13}}{detM}(-\omega M_q) + \frac{M_{33}}{detM}(-\omega L_q) + \frac{M_{53}}{detM}(-\omega M_q),\ F_{35} = \frac{M_{53}}{detM}R,\ F_{36} = \frac{M_{13}}{detM}(-\omega M_q) + \frac{M_{33}}{detM}(-\omega M_q) + \frac{M_{53}}{detM}(-\omega L_q).$

$F_{41} = \frac{M_{24}}{detM}(\omega L_d) + \frac{M_{44}}{detM}(\omega M_d) + \frac{M_{64}}{detM}(\omega M_d),\ F_{42} = 0,\ F_{43} = \frac{M_{24}}{detM}(\omega M_d) + \frac{M_{44}}{detM}(\omega L_d) + \frac{M_{64}}{detM}(\omega M_d),$ $F_{44} = 0,\ F_{45} = \frac{M_{24}}{detM}(\omega M_d) + \frac{M_{44}}{detM}(\omega M_d) + \frac{M_{64}}{detM}(\omega L_d),\ F_{46} = 0.$

$F_{51} = \frac{M_{15}}{detM}R,\ F_{52} = \frac{M_{15}}{detM}(-\omega L_q) + \frac{M_{35}}{detM}(-\omega M_q) + \frac{M_{55}}{detM}(-\omega M_q),\ F_{53} = \frac{M_{35}}{detM}R,\ F_{55} = \frac{M_{15}}{detM}(-\omega M_q) + \frac{M_{35}}{detM}(-\omega L_q) + \frac{M_{55}}{detM}(-\omega M_q),\ F_{55} = \frac{M_{55}}{detM}R,\ F_{56} = \frac{M_{15}}{detM}(-\omega M_q) + \frac{M_{35}}{detM}(-\omega M_q) + \frac{M_{55}}{detM}(-\omega L_q).$

$F_{61} = \frac{M_{26}}{} detM(\omega L_d) + \frac{M_{46}}{detM}(\omega M_d) + \frac{M_{66}}{detM}(\omega M_d),\ F_{62} = 0,\ F_{63} = \frac{M_{26}}{detM}(\omega M_d) + \frac{M_{46}}{detM}(\omega L_d) + \frac{M_{66}}{detM}(\omega M_d),$ $F_{64} = 0,\ F_{65} = \frac{M_{26}}{detM}(\omega M_d) + \frac{M_{46}}{detM}(\omega M_d) + \frac{M_{66}}{detM}(\omega L_d),\ F_{66} = 0.$

About the rotational motion of the 9-phase PMSM, this is caused by the aggregate electromagnetic torque of the motor which is given by:

$$\begin{array}{c} T_e = \frac{3}{2}p[\Psi_m(i_{q1} + i_{q2} + i_{q3}) + (i_{d1}i_{q1} + i_{d2}i_{q2} + i_{d3}i_{q3})(L_d - L_q) + \\ +(i_{d1}i_{q2} + i_{d2}i_{q1} + i_{d1}i_{q3} + i_{d3}i_{q1} + i_{d2}i_{q3} + i_{d3}i_{q2})(M_d - M_q)] \end{array} \quad (18)$$

The turn motion of the motor is described by

$$\begin{array}{c} \dot{\theta} = \omega \\ \dot{\omega} = \frac{1}{J}[T_e - T_L - b\omega] \end{array} \quad (19)$$

where one can consider that the torque due to load T_L is a function of the turn angle θ, for instance $T_L = mgl_1 sin(\theta)$ in the case of lifting a mass m attached to the end of a rod of link l_1.

The state variables of the 9-phase PMSM are defined as $x_1 = \theta$, $x_2 = \omega$, $x_3 = i_{d1}$, $x_4 = i_{q1}$, $x_5 = i_{d2}$, $x_6 = i_{q2}$, $x_7 = i_{d3}$, $x_8 = i_{q3}$. Using the above notation, the state-space model of the 9-phase PMSM becomes

$$\begin{gathered}\dot{x}_1 = x_2 \\ \dot{x}_2 = \frac{1}{J}\{\frac{3}{2}p[\Psi_m(x_4+x_6+x_8) + (x_3x_4+x_5x_6+x_7x_8)(L_d-L_q)+ \\ +(x_3x_6+x_5x_4+x_3x_8+x_7x_4+x_5x_8+x_7x_6)(M_d-M_q)]- \\ -mgl_1 sin(x_1) - bx_2\}\end{gathered} \tag{20}$$

while about the electrical part of the 9-phase PMSM one has

$$\begin{pmatrix}\dot{x}_3\\ \dot{x}_4\\ \dot{x}_5\\ \dot{x}_6\\ \dot{x}_7\\ \dot{x}_8\end{pmatrix} = -\begin{pmatrix}F_{11} & F_{12} & F_{13} & F_{14} & F_{15} & F_{16}\\ F_{21} & F_{22} & F_{23} & F_{24} & F_{25} & F_{26}\\ F_{31} & F_{32} & F_{33} & F_{34} & F_{35} & F_{36}\\ F_{41} & F_{42} & F_{43} & F_{44} & F_{45} & F_{46}\\ F_{51} & F_{52} & F_{53} & F_{54} & F_{55} & F_{56}\\ F_{61} & F_{62} & F_{63} & F_{64} & F_{65} & F_{66}\end{pmatrix}\begin{pmatrix}x_3\\ x_4\\ x_5\\ x_6\\ x_7\\ x_8\end{pmatrix} + \begin{pmatrix}\frac{M_{11}}{detM} & 0 & \frac{M_{31}}{detM} & 0 & \frac{M_{51}}{detM} & 0\\ 0 & \frac{M_{22}}{detM} & 0 & \frac{M_{42}}{detM} & 0 & \frac{M_{62}}{detM}\\ \frac{M_{13}}{detM} & 0 & \frac{M_{33}}{detM} & 0 & \frac{M_{53}}{detM} & 0\\ 0 & \frac{M_{24}}{detM} & 0 & \frac{M_{44}}{detM} & 0 & \frac{M_{64}}{detM}\\ \frac{M_{15}}{detM} & 0 & \frac{M_{35}}{detM} & 0 & \frac{M_{55}}{detM} & 0\\ 0 & \frac{M_{26}}{detM} & 0 & \frac{M_{46}}{detM} & 0 & \frac{M_{66}}{detM}\end{pmatrix}\begin{pmatrix}u_1\\ u_2\\ u_3\\ u_4\\ u_5\\ u_6\end{pmatrix} \tag{21}$$

The following drift vector is defined for the 9-phase PMSM

$$f(x) = \begin{pmatrix}f_1(x) & f_2(x) & f_3(x) & f_4(x) & f_5(x) & f_6(x) & f_7(x) & f_8(x)\end{pmatrix}^T \tag{22}$$

where the elements of the drift vector are defined as follows:

$$f_1(x) = x_2 \tag{23}$$

$$\begin{gathered}f_2(x) = \frac{1}{J}\{\frac{3}{2}p[\Psi_m(x_4+x_6+x_8) + (x_3x_4+x_5x_6+x_7x_8)(L_d-L_q)+ \\ +(x_3x_6+x_5x_4+x_3x_8+x_7x_4+x_5x_8+x_7x_6)(M_d-M_q)]- \\ -mgl_1 sin(x_1) - bx_2\end{gathered} \tag{24}$$

$$f_3(x) = -(F_{11}x_3 + F_{12}x_4 + F_{13}x_5 + F_{14}x_6 + F_{15}x_7 + F_{16}x_8) \tag{25}$$

$$f_4(x) = -(F_{21}x_3 + F_{22}x_4 + F_{23}x_5 + F_{24}x_6 + F_{25}x_7 + F_{26}x_8) \tag{26}$$

$$f_5(x) = -(F_{31}x_3 + F_{32}x_4 + F_{33}x_5 + F_{34}x_6 + F_{35}x_7 + F_{36}x_8) \tag{27}$$

$$f_7(x) = -(F_{51}x_3 + F_{52}x_4 + F_{53}x_5 + F_{54}x_6 + F_{55}x_7 + F_{56}x_8) \tag{28}$$

$$f_7(x) = -(F_{51}x_3 + F_{52}x_4 + F_{53}x_5 + F_{54}x_6 + F_{55}x_7 + F_{56}x_8) \tag{29}$$

$$f_8(x) = -(F_{61}x_3 + F_{62}x_4 + F_{63}x_5 + F_{64}x_6 + F_{65}x_7 + F_{66}x_8) \tag{30}$$

Additionally, based on the control inputs gain matrix $g(x) = M^{-1}$ one defines the following control input gain vectors

$$g_1(x) = \begin{pmatrix}0\\ 0\\ \frac{M_{11}}{detM}\\ 0\\ \frac{M_{13}}{detM}\\ 0\\ \frac{M_{15}}{detM}\\ 0\end{pmatrix} \quad g_2(x) = \begin{pmatrix}0\\ 0\\ 0\\ \frac{M_{22}}{detM}\\ 0\\ \frac{M_{24}}{detM}\\ 0\\ \frac{M_{26}}{detM}\end{pmatrix} \quad g_3(x) = \begin{pmatrix}0\\ 0\\ \frac{M_{31}}{detM}\\ 0\\ \frac{M_{33}}{detM}\\ 0\\ \frac{M_{35}}{detM}\\ 0\end{pmatrix} \quad g_4(x) = \begin{pmatrix}0\\ 0\\ 0\\ \frac{M_{42}}{detM}\\ 0\\ \frac{M_{44}}{detM}\\ 0\\ \frac{M_{46}}{detM}\end{pmatrix} \quad g_5(x) = \begin{pmatrix}0\\ 0\\ \frac{M_{51}}{detM}\\ 0\\ \frac{M_{53}}{detM}\\ 0\\ \frac{M_{55}}{detM}\\ 0\end{pmatrix} \quad g_6(x) = \begin{pmatrix}0\\ 0\\ 0\\ \frac{M_{62}}{detM}\\ 0\\ \frac{M_{64}}{detM}\\ 0\\ \frac{M_{66}}{detM}\end{pmatrix} \tag{31}$$

Concisely, the dynamic model of the 9-phase PMSM can be written in the following affine-in-the-input state-space form

$$\dot{z} = f(x) + g_1(x)u_1 + g_2(x)u_2 + g_3(x)u_3 + g_4(x)u_4 + g_5(x)u_5 + g_6(x)u_6 \tag{32}$$

where $x \in R^{8\times 1},\ f(x) \in R^{8\times 1},\ g_i(x) \in R^{8\times 1}$ for $i = 1, 2, \cdots, 6$ and $u_i \in R$ for $i = 1, 2, \cdots, 6$. The diagram of the nine-phase PMSM which is fed by a nine-phase Voltage Source Inverter is shown in Fig. 2.

The dynamic model of the 9-phase PMSM can be controlled by three separate 3-phase inverters. Each one of these inverters will be dedicated to modify the AC current and voltage variables of one of the 3-phase reference frames of the nine-phase motor. The dynamic model the 3-phase inverters has been analyzed in several research articles and monographs, as for instance in (Rigatos, 2016), (Rigatos, Abbaszadeh and Hamida, 2023), Moreover, in (Rigatos, 2016), (Rigatos, Abbaszadeh and Hamida, 2023) the control problem of three-phase inverters has been dealt with several methods (i) global linearization-based control (Lie algebra-based control and flatness-based control through transformation into canonical forms), (ii) approximate linearization-based control (nonlinear optimal control), (iii) Lyapunov theory-based control (adaptive control schemes), (iv) other nonlinear control methods (sliding-mode control, flatness-based control in successive loops). The control inputs of the inverter are generated with the use of the pulse-width-modulation (PWM) technique. The joint inverter and 9-phase PMSM system can be controlled into consecutive loops. The control inputs of the 9-phase PMSM which are computed through the article's nonlinear optimal control method become setpoints for the three inverters that inject control currents to the phases of the motor (Rigatos, 2016), (Rigatos, Abbaszadeh and Hamida, 2023).

As noted before, a triple three-phase notation is considered for the motor's voltages and currents, which is given as $(a_1, b_1, c_1),\ (a_2, b_2, c_2)$, and (a_3, b_3, c_3). After applying Clarke's and Park's transformations to each one of the three 3-phase *abc* frames of the 9-phase PMSM these are turned into three 2-phase *dq* frames which are synchronously rotating with the motor and which are denoted as $(d_1, q_1),\ (d_2, q_2)$ and (d_3, q_3). To obtain AC current waveforms, associated with the phases of the 9-phase PMSM one has to use the inverse of the transformation matrix $\bar{M}$ that connects the initial description of the currents of the motor from three 3-phase systems $(a_1, b_1, c_1),\ (a_2, b_2, c_2),\ (a_3, b_3, c_3)$ into the three 2-phase systems $(d_1, q_1),\ (d_2, q_2),\ (d_3, q_3)$. By mutiplying this inverse matrix, which is noted as $\bar{M}^{-1}$, with the vector of the current state variables $[i_{d1}, i_{q1}]^T$, $[i_{d2}, i_{q2}]^T$, and $[i_{d3}, i_{q3}]^T$, which are computed by the article's nonlinear optimal control method one obtains the AC current waveforms of the 9-phase PMSM.

The forward transformation matrix that allows to turn a current or voltage vector of the first *abc* 3-phase frame into a current or voltage vector of the first *dq* frame is denoted below as $\bar{M}$,

$$\bar{M} = \frac{2}{3}\begin{pmatrix} cos(\theta) & cos(\theta - \frac{2\pi}{3}) & cos(\theta + \frac{2\pi}{3}) \\ -sin(\theta) & -sin(\theta - \frac{2\pi}{3}) & -sin(\theta + \frac{2\pi}{3}) \\ \frac{1}{2} & \frac{1}{2} & \frac{1}{2} \end{pmatrix} \tag{33}$$

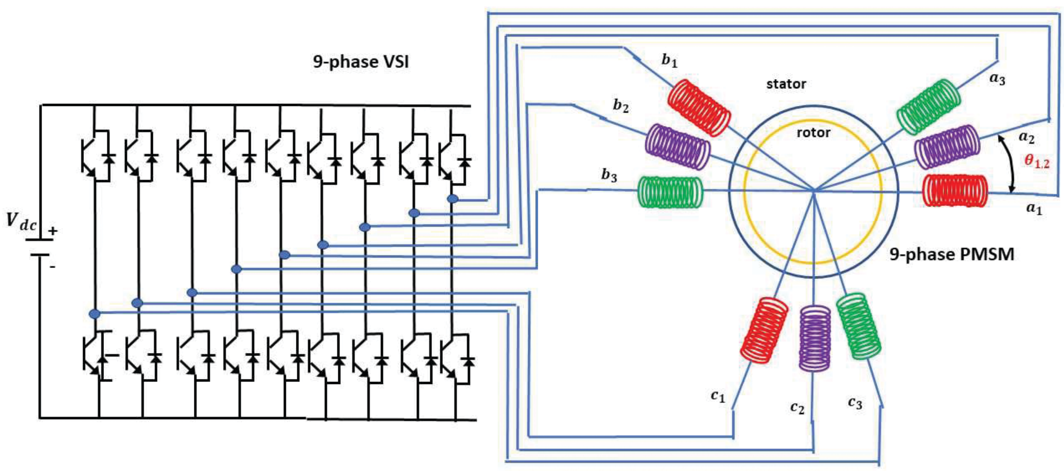

Fig. 2. Diagram of the 9-phase PMSM driven by a voltage source inverter.

while its inverse matrix which allows to turn a current or voltage vector of the first dq 2-phase frame into a current or voltage vector for the first abc 3-phase frame is denoted below as $\bar{M}^{-1}$

$$\bar{M}^{-1} = \begin{pmatrix} cos(\theta) & -sin(\theta) & 1 \\ cos(\theta-\frac{2\pi}{3}) & -sin(\theta-\frac{2\pi}{3}) & 1 \\ cos(\theta+\frac{2\pi}{3}) & -sin(\theta+\frac{2\pi}{3}) & 1 \end{pmatrix} \tag{34}$$

Considering that the 3-phase reference frames of the nine-phase PMSM are shifted between them by an angle equal to a then a phase coefficient of $\pm\frac{2\pi}{3}+a$ will have be used in the transformation matrices of the second 3-phase frame, while a phase coefficient of $\pm\frac{2\pi}{3}+2a$ will have be used in the transformation matrices of the third 3-phase frame.

3. Differential flatness properties of the 9-phase PMSM

It will be proven that the dynamic model of the nine-phase PMSM is differentially flat with flat outputs vector $Y=[y_1,y_2,y_3,y_4,y_5,y_6]^T$ or $Y=[x_1,x_3,x_5,x_6,x_7,x_9]^T$. From the first row of the state-space model one has

$$x_2=\dot{x}_1 \Rightarrow x_2=h_2(Y,\dot{Y}) \tag{35}$$

which signifies that x_2 is a differential function of the flat outputs vector. From the second row of the state-space model one can also solve for state variable x_4

$$\begin{array}{c} \dot{x}_2-\frac{1}{J}\{\frac{3}{2}p[\Psi_m(x_6+x_8)+(x_5x_6+x_7x_8)(L_d-L_q)+ \\ +(x_3x_6+x_3x_8+x_5x_8+x_7x_6)(M_d-M_q)]-mgLsin(x_1)-bx_2\}= \\ =\frac{1}{J}\frac{3}{2}p[\Psi_m+x_3(L_d-L_q)+(x_5+x_7)(M_d-M_q)]x_4 \end{array} \tag{36}$$

Next, by denoting functions $q_1(x)$ and $q_2(x)$ as follows

$$\begin{array}{c} q_1(x)=\dot{x}_2-\frac{1}{J}\{\frac{3}{2}p[\Psi_m(x_6+x_8)+(x_5x_6+x_7x_8)(L_d-L_q)+ \\ +(x_3x_6+x_3x_8+x_5x_8+x_7x_6)(M_d-M_q)]-mgLsin(x_1)-bx_2\} \end{array} \tag{37}$$

$$q_2(x)=\frac{1}{J}\frac{3}{2}p[\Psi_m+x_3(L_d-L_q)+(x_5+x_7)(M_d-M_q)] \tag{38}$$

and by solving for x_4 one has

$$x_4=\frac{q_1(x)}{q_2(x)} \Rightarrow x_4=h_4(Y,\dot{Y}) \tag{39}$$

which signifies that state variable x_4 is also a differential function of the flat outputs of the system.

Moreover, from rows 3 to 8 of the state-space model one has

$$\dot{x}_{3,8}=-F{\cdot}x_{3,8}+Gu \tag{40}$$

where $x_{3,8}=[x_3,x_4,x_5,x_6,x_7,x_8]^T$ while matrices F and G are given by

$$F=\begin{pmatrix} F_{11} & F_{12} & F_{13} & F_{14} & F_{15} & F_{16} \\ F_{21} & F_{22} & F_{23} & F_{24} & F_{25} & F_{26} \\ F_{31} & F_{32} & F_{33} & F_{34} & F_{35} & F_{36} \\ F_{41} & F_{42} & F_{43} & F_{44} & F_{45} & F_{46} \\ F_{51} & F_{52} & F_{53} & F_{54} & F_{55} & F_{56} \\ F_{61} & F_{62} & F_{63} & F_{64} & F_{65} & F_{66} \end{pmatrix} \quad G=\begin{pmatrix} \frac{M_{11}}{detM} & 0 & \frac{M_{31}}{detM} & 0 & \frac{M_{51}}{detM} & 0 \\ 0 & \frac{M_{22}}{detM} & 0 & \frac{M_{42}}{detM} & 0 & \frac{M_{62}}{detM} \\ \frac{M_{13}}{detM} & 0 & \frac{M_{33}}{detM} & 0 & \frac{M_{53}}{detM} & 0 \\ 0 & \frac{M_{24}}{detM} & 0 & \frac{M_{44}}{detM} & 0 & \frac{M_{64}}{detM} \\ \frac{M_{15}}{detM} & 0 & \frac{M_{35}}{detM} & 0 & \frac{M_{55}}{detM} & 0 \\ 0 & \frac{M_{26}}{detM} & 0 & \frac{M_{46}}{detM} & 0 & \frac{M_{66}}{detM} \end{pmatrix} \tag{41}$$

By solving the previous equation for the control inputs vector *u* one obtains

$$u = G^{-1}[\dot{x}_{3,8} + F{\cdot}x_{3,8}] \Rightarrow u = h_u(Y, \dot{Y}) \tag{42}$$

which signifies that the control inputs vector is also a differential function of the flat outputs vector of the system. Therefore, the entire dynamic model of the 9-phase PMSM is differentially flat.

The differential flatness property signifies that the model of the 9-phase PMSM is input-output linearizable. Besides, it allows to solve the associated setpoints definition problem. Setpoints are defined in unconditional manner for those state variables which coincide with the flat outputs of the system. For the rest of the state variables, setpoints are chosen as differential functions of the setpoints of the flat outputs.

4. Approximate linearization of the dynamic model of the 9-phase PMSM

The dynamic model of the 9-phase PMSM being initially in the state-space form $\dot{x} = f(x) + g(x)u$ or $\dot{x} = f(x) + \sum_{i=1}^{6} g_i(x)u_i$ undergoes approximate linearization through first-order Taylor series expansion and through the computation of the associated Jacobian matrices. The linearization point is updated at each sampling instance and is denoted as (x^*, u^*), where x^* is the present value of the system's state vector and u^* is the last sampled value of the control inputs vector. This results into the linear state-space form

$$\dot{x} = Ax + Bu + \tilde{d} \tag{43}$$

where A, B are the Jacobian matrices of the system and $\tilde{d}$ is the cumulative disturbance term which may include: (i) modelling error due to the truncation of higher-order terms in the Taylor series expansion, (ii) exogenous perturbations (iii) sensor noise of any distribution. Since the elements of the columns of the control inputs gain matrix *g*(*x*) are constants, the Jacobian matrices of the system are defined as follows:

$$A = \nabla_x[f(x) + g(x)u] \mid_{(x^*,u^*)} \Rightarrow A = \nabla_x f(x) \mid_{(x^*,u^*)} \tag{44}$$

$$B = \nabla_u[f(x) + g(x)u] \mid_{(x^*,u^*)} \Rightarrow B = g(x) \mid_{(x^*,u^*)} \tag{45}$$

This linearization approach which has been followed for implementing the nonlinear optimal control scheme results into a quite accurate model of the system's dynamics. Consider for instance the following affine-in-the-input state-space model

$$\begin{gathered}\dot{x} = f(x) + g(x)u \Rightarrow \\ \dot{x} = [f(x^*) + \nabla_x f(x) \mid_{x^*} (x - x^*)] + [g(x^*) + \nabla_x g(x) \mid_{x^*} (x - x^*)]u^* + g(x^*)u^* + g(x^*)(u - u^*) + \tilde{d}_1 \Rightarrow \\ \dot{x} = [\nabla_x f(x) \mid_{x^*} + \nabla_x g(x) \mid_{x^*} u^*]x + g(x^*)u - [\nabla_x f(x) \mid_{x^*} + \nabla_x g(x) \mid_{x^*} u^*]x^* + f(x^*) + g(x^*)u^* + \tilde{d}_1\end{gathered} \tag{46}$$

where $\tilde{d}_1$ is the modelling error due to truncation of higher order terms in the Taylor series expansion of $f(x)$ and $g(x)$. Next, by defining $A = [\nabla_x f(x) \mid_{x^*} + \nabla_x g(x) \mid_{x^*} u^*]$, $B = g(x^*)$ one obtains

$$\dot{x} = Ax + Bu - Ax^* + f(x^*) + g(x^*)u^* + \tilde{d}_1 \tag{47}$$

Moreover by denoting $\tilde{d} = -Ax^* + f(x^*) + g(x^*)u^* + \tilde{d}_1$ about the cumulative modelling error term in the Taylor series expansion procedure one has

$$\dot{x} = Ax + Bu + \tilde{d} \tag{48}$$

which is the approximately linearized model of the dynamics of the system of Eq. (43). The term $f(x^*) + g(x^*)u^*$ is the derivative of the state vector at (x^*, u^*) which is almost annihilated by $-Ax^*$.

The computation of the Jacobian matrix $A=\nabla_x[f(x)+g(x)u]\mid_{(x^*,u^*)}$ proceeds as follows:

First row of the Jacobian matrix $A=\nabla_x[f(x)+g(x)u]\mid_{(x^*,u^*)}$: $\frac{\partial f_1}{\partial x_1}=0$, $\frac{\partial f_1}{\partial x_2}=1$, $\frac{\partial f_1}{\partial x_3}=0$, $\frac{\partial f_1}{\partial x_4}=0$, $\frac{\partial f_1}{\partial x_5}=0$, $\frac{\partial f_1}{\partial x_6}=0$, $\frac{\partial f_1}{\partial x_7}=0$, $\frac{\partial f_1}{\partial x_8}=0$.

Second row of the Jacobian matrix $A=\nabla_x[f(x)+g(x)u]\mid_{(x^*,u^*)}$: $\frac{\partial f_2}{\partial x_1}=-\frac{1}{J}mgLcos(x_1)$, $\frac{\partial f_2}{\partial x_2}=-\frac{b}{J}$, $\frac{\partial f_2}{\partial x_3}=\frac{1}{J}\{\frac{3}{2}p[x_4(L_d-L_q)+(x_6+x_8)(M_d-M_q)]\}$, $\frac{\partial f_2}{\partial x_4}=\frac{1}{J}\{\frac{3}{2}p[\Psi_m+x_3(L_d-L_q)+(x_5+x_7)(M_d-M_q)]\}$, $\frac{\partial f_2}{\partial x_5}=\frac{1}{J}\{\frac{3}{2}p[x_6(L_d-L_q)+(x_4+x_8)(M_d-M_q)]\}$, $\frac{\partial f_2}{\partial x_6}=\frac{1}{J}\{\frac{3}{2}p[\Psi_m+x_5(L_d-L_q)+(x_3+x_7)(M_d-M_q)]\}$, $\frac{\partial f_2}{\partial x_7}=\frac{1}{J}\{\frac{3}{2}p[x_8(L_d-L_q)+(x_4+x_6)(M_d-M_q)]\}$, $\frac{\partial f_2}{\partial x_8}=\frac{1}{J}\{\frac{3}{2}p[\Psi_m+x_7(L_d-L_q)+(x_3+x_5)(M_d-M_q)]\}$.

Third row of the Jacobian matrix $A=\nabla_x[f(x)+g(x)u]\mid_{(x^*,u^*)}$: $\frac{\partial f_3}{\partial x_1}=0$, $\frac{\partial f_3}{\partial x_2}=-[\frac{\partial F_{11}}{\partial x_2}x_3+\frac{\partial F_{12}}{\partial x_2}x_4+\frac{\partial F_{13}}{\partial x_2}x_5+\frac{\partial F_{14}}{\partial x_2}x_6+\frac{\partial F_{15}}{\partial x_2}x_7+\frac{\partial F_{16}}{\partial x_2}x_8]$, $\frac{\partial f_3}{\partial x_3}=-F_{11}$, $\frac{\partial f_3}{\partial x_4}=-F_{12}$, $\frac{\partial f_3}{\partial x_5}=-F_{13}$, $\frac{\partial f_3}{\partial x_6}=-F_{14}$, $\frac{\partial f_3}{\partial x_7}=-F_{15}$, $\frac{\partial f_3}{\partial x_8}=-F_{16}$.

Fourth row of the Jacobian matrix $A=\nabla_x[f(x)+g(x)u]\mid_{(x^*,u^*)}$: $\frac{\partial f_4}{\partial x_1}=0$, $\frac{\partial f_4}{\partial x_2}=-[\frac{\partial F_{21}}{\partial x_2}x_3+\frac{\partial F_{22}}{\partial x_2}x_4+\frac{\partial F_{23}}{\partial x_2}x_5+\frac{\partial F_{24}}{\partial x_2}x_6+\frac{\partial F_{25}}{\partial x_2}x_7+\frac{\partial F_{26}}{\partial x_2}x_8]$, $\frac{\partial f_4}{\partial x_3}=-F_{21}$, $\frac{\partial f_4}{\partial x_4}=-F_{22}$, $\frac{\partial f_4}{\partial x_5}=-F_{23}$, $\frac{\partial f_4}{\partial x_6}=-F_{24}$, $\frac{\partial f_4}{\partial x_7}=-F_{25}$, $\frac{\partial f_4}{\partial x_8}=-F_{26}$.

Fifth row of the Jacobian matrix $A=\nabla_x[f(x)+g(x)u]\mid_{(x^*,u^*)}$: $\frac{\partial f_5}{\partial x_1}=0$, $\frac{\partial f_5}{\partial x_2}=-[\frac{\partial F_{31}}{\partial x_2}x_3+\frac{\partial F_{32}}{\partial x_2}x_4+\frac{\partial F_{33}}{\partial x_2}x_5+\frac{\partial F_{34}}{\partial x_2}x_6+\frac{\partial F_{35}}{\partial x_2}x_7+\frac{\partial F_{36}}{\partial x_2}x_8]$, $\frac{\partial f_5}{\partial x_3}=-F_{31}$, $\frac{\partial f_5}{\partial x_4}=-F_{32}$, $\frac{\partial f_5}{\partial x_5}=-F_{33}$, $\frac{\partial f_5}{\partial x_6}=-F_{34}$, $\frac{\partial f_5}{\partial x_7}=-F_{35}$, $\frac{\partial f_5}{\partial x_8}=-F_{36}$.

Sixth row of the Jacobian matrix $A=\nabla_x[f(x)+g(x)u]\mid_{(x^*,u^*)}$: $\frac{\partial f_6}{\partial x_1}=0$, $\frac{\partial f_6}{\partial x_2}=-[\frac{\partial F_{41}}{\partial x_2}x_3+\frac{\partial F_{42}}{\partial x_2}x_4+\frac{\partial F_{43}}{\partial x_2}x_5+\frac{\partial F_{44}}{\partial x_2}x_6+\frac{\partial F_{45}}{\partial x_2}x_7+\frac{\partial F_{46}}{\partial x_2}x_8]$, $\frac{\partial f_6}{\partial x_3}=-F_{41}$, $\frac{\partial f_6}{\partial x_4}=-F_{42}$, $\frac{\partial f_6}{\partial x_5}=-F_{43}$, $\frac{\partial f_6}{\partial x_6}=-F_{44}$, $\frac{\partial f_6}{\partial x_7}=-F_{45}$, $\frac{\partial f_6}{\partial x_8}=-F_{46}$.

Seventh row of the Jacobian matrix $A=\nabla_x[f(x)+g(x)u]\mid_{(x^*,u^*)}$: $\frac{\partial f_7}{\partial x_1}=0$, $\frac{\partial f_7}{\partial x_2}=-[\frac{\partial F_{51}}{\partial x_2}x_3+\frac{\partial F_{52}}{\partial x_2}x_4+\frac{\partial F_{53}}{\partial x_2}x_5+\frac{\partial F_{54}}{\partial x_2}x_6+\frac{\partial F_{55}}{\partial x_2}x_7+\frac{\partial F_{56}}{\partial x_2}x_8]$, $\frac{\partial f_7}{\partial x_3}=-F_{51}$, $\frac{\partial f_7}{\partial x_4}=-F_{52}$, $\frac{\partial f_7}{\partial x_5}=-F_{53}$, $\frac{\partial f_7}{\partial x_6}=-F_{54}$, $\frac{\partial f_7}{\partial x_7}=-F_{55}$, $\frac{\partial f_7}{\partial x_8}=-F_{56}$.

Eighth row of the Jacobian matrix $A=\nabla_x[f(x)+g(x)u]\mid_{(x^*,u^*)}$: $\frac{\partial f_8}{\partial x_1}=0$, $\frac{\partial f_8}{\partial x_2}=-[\frac{\partial F_{61}}{\partial x_2}x_3+\frac{\partial F_{62}}{\partial x_2}x_4+\frac{\partial F_{63}}{\partial x_2}x_5+\frac{\partial F_{64}}{\partial x_2}x_6+\frac{\partial F_{65}}{\partial x_2}x_7+\frac{\partial F_{66}}{\partial x_2}x_8]$, $\frac{\partial f_8}{\partial x_3}=-F_{61}$, $\frac{\partial f_8}{\partial x_4}=-F_{62}$, $\frac{\partial f_8}{\partial x_5}=-F_{63}$, $\frac{\partial f_8}{\partial x_6}=-F_{64}$, $\frac{\partial f_8}{\partial x_7}=-F_{65}$, $\frac{\partial f_8}{\partial x_8}=-F_{66}$.

where it has been used that; $\frac{\partial F_{11}}{\partial x_2}=0$, $\frac{\partial F_{12}}{\partial x_2}=\frac{M_{11}}{detM}(-L_q)+\frac{M_{31}}{detM}(-M_q)+\frac{M_{51}}{detM}(-M_q)$, $\frac{\partial F_{13}}{\partial x_2}=0$, $\frac{\partial F_{14}}{\partial x_2}=\frac{M_{11}}{detM}(-M_q)+\frac{M_{31}}{detM}(-L_q)+\frac{M_{51}}{detM}(-M_q)$, $\frac{\partial F_{15}}{\partial x_2}=0$ $\frac{\partial F_{16}}{\partial x_2}=\frac{M_{11}}{detM}(-M_q)+\frac{M_{31}}{detM}(-M_q)+\frac{M_{51}}{detM}(-L_q)$.

Additionally one has that $\frac{\partial F_{21}}{\partial x_2}=\frac{M_{22}}{detM}(L_d)+\frac{M_{42}}{detM}(M_d)+\frac{M_{62}}{detM}(M_d)$, $\frac{\partial F_{22}}{\partial x_2}=0$, $\frac{\partial F_{23}}{\partial x_2}=\frac{M_{22}}{detM}(M_d)+\frac{M_{42}}{detM}(L_d)+\frac{M_{62}}{detM}(M_d)$, $\frac{\partial F_{24}}{\partial x_2}=0$, $\frac{\partial F_{25}}{\partial x_2}=\frac{M_{22}}{detM}(M_d)+\frac{M_{42}}{detM}(M_d)+\frac{M_{62}}{detM}(L_d)$, $\frac{\partial F_{26}}{\partial x_2}=0$

Furthermore $\frac{\partial F_{31}}{\partial x_2}=0$, $\frac{\partial F_{32}}{\partial x_2}=\frac{M_{13}}{detM}(-L_q)+\frac{M_{33}}{detM}(-M_q)+\frac{M_{53}}{detM}(-M_q)$, $\frac{\partial F_{33}}{\partial x_2}=0$, $\frac{\partial F_{34}}{\partial x_2}=\frac{M_{13}}{detM}(-M_q)+\frac{M_{33}}{detM}(-L_q)+\frac{M_{53}}{detM}(-M_q)$, $\frac{\partial F_{35}}{\partial x_2}=0$ $\frac{\partial F_{36}}{\partial x_2}=\frac{M_{13}}{detM}(-M_q)+\frac{M_{33}}{detM}(-M_q)+\frac{M_{53}}{detM}(-L_q)$.

Moreover one has that $\frac{\partial F_{41}}{\partial x_2}=\frac{M_{24}}{detM}(L_d)+\frac{M_{44}}{detM}(M_d)+\frac{M_{64}}{detM}(M_d)$, $\frac{\partial F_{42}}{\partial x_2}=0$, $\frac{\partial F_{43}}{\partial x_2}=\frac{M_{24}}{detM}(M_d)+\frac{M_{44}}{detM}(L_d)+\frac{M_{64}}{detM}(M_d)$, $\frac{\partial F_{44}}{\partial x_2}=0$, $\frac{\partial F_{45}}{\partial x_2}=\frac{M_{24}}{detM}(M_d)+\frac{M_{44}}{detM}(M_d)+\frac{M_{64}}{detM}(L_d)$, $\frac{\partial F_{46}}{\partial x_2}=0$.

Additionally $\frac{\partial F_{51}}{\partial x_2}=0$, $\frac{\partial F_{52}}{\partial x_2}=\frac{M_{15}}{detM}(-L_q)+\frac{M_{35}}{detM}(-M_q)+\frac{M_{55}}{detM}(-M_q)$, $\frac{\partial F_{53}}{\partial x_2}=0$, $\frac{\partial F_{54}}{\partial x_2}=\frac{M_{15}}{detM}(-M_q)+\frac{M_{35}}{detM}(-L_q)+\frac{M_{55}}{detM}(-M_q)$, $\frac{\partial F_{55}}{\partial x_2}=0$ $\frac{\partial F_{56}}{\partial x_2}=\frac{M_{15}}{detM}(-M_q)+\frac{M_{35}}{detM}(-M_q)+\frac{M_{55}}{detM}(-L_q)$

Finally one has that $\frac{\partial F_{61}}{\partial x_2}=\frac{M_{26}}{detM}(L_d)+\frac{M_{46}}{detM}(M_d)+\frac{M_{66}}{detM}(M_d)$, $\frac{\partial F_{62}}{\partial x_2}=0$, $\frac{\partial F_{63}}{\partial x_2}=\frac{M_{26}}{detM}(M_d)+\frac{M_{46}}{detM}(L_d)+\frac{M_{66}}{detM}(M_d)$, $\frac{\partial F_{64}}{\partial x_2}=0$, $\frac{\partial F_{65}}{\partial x_2}=\frac{M_{26}}{detM}(M_d)+\frac{M_{46}}{detM}(M_d)+\frac{M_{66}}{detM}(L_d)$, $\frac{\partial F_{66}}{\partial x_2}=0$.

5. Desing of a stabilizing H-infinity feedback controller

5.1 Min-max control and disturbance rejection

In the H_∞ control approach, a feedback control scheme is designed for setpoint tracking by the system's state vector and simultaneous disturbance rejection, considering that the disturbance affects the system in the worst possible manner. For the approximately linearized model of Eq. (43), the disturbances' effects are incorporated in the following quadratic cost function (Rigatos, 2016)

$$J(t)=\frac{1}{2}\int_0^T[y^T(t)y(t)+ru^T(t)u(t)-\rho^2\tilde{d}^T(t)\tilde{d}(t)]dt,\quad r,\rho>0 \tag{49}$$

The significance of the negative sign in the cost function's term that is associated with the perturbation variable $\tilde{d}(t)$ is that the disturbance tries to maximize the cost function $J(t)$ while the control signal $u(t)$ tries to minimize it.

The physical meaning of the relation given above is that the control signal and the disturbances compete to each other within a min-max differential game. This problem of min-max optimization can be written as $min_u max_{\tilde{d}} J(u,\tilde{d})$. The objective of the optimization procedure is to compute a control signal $u(t)$ which can compensate for the worst possible disturbance that affects the system. However, the solution to the min-max optimization problem is directly related to the value of parameter ρ. This means that there is an upper bound in the disturbances magnitude that can be annihilated by the control signal.

5.2 Design of the stabilizing feedback controller

After linearization around its current operating point (x^*,u^*), the dynamic model of the 9-phase PMSM is written as

$$\dot{x}=Ax+Bu+d_1 \tag{50}$$

Parameter d_1 stands for the linearization error in the 9-phase PMSM's model appearing previously in Eq. (50). The reference setpoints for the state vector of the nine-phase PMSM are denoted by $\mathbf{x_d}=[x_1^d,\cdots,x_8^d]$. Tracking of this trajectory is achieved after applying the control input u_d. At every time instant the control input u_d is assumed to differ from the control input u appearing in Eq. (50) by an amount equal to Δu, that is $u_d=u+\Delta u$

$$\dot{x}_d=Ax_d+Bu_d+d_2 \tag{51}$$

The dynamics of the controlled system described in Eq. (50) can be also written as

$$\dot{x}=Ax+Bu+Bu_d-Bu_d+d_1 \tag{52}$$

and by denoting $d_3=-Bu_d+d_1$ as an aggregate disturbance term one obtains

$$\dot{x}=Ax+Bu+Bu_d+d_3 \tag{53}$$

By subtracting Eq. (51) from Eq. (53) one has

$$\dot{x} - \dot{x}_d = A(x - x_d) + Bu + d_3 - d_2 \tag{54}$$

By denoting the tracking error as $e = x - x_d$ and the aggregate disturbance term as $L\tilde{d} = d_3 - d_2$, the tracking error dynamics becomes

$$\dot{e} = Ae + Bu + L\tilde{d} \tag{55}$$

with L to be representing the disturbance inputs gain matrix. For the linearized system the cost function of Eq. (49) is defined, where coefficient r determines the penalization of the control input and the weight coefficient ρ determines the reward of the disturbances' effects. Then, the optimal feedback control law is given by

$$u(t) = -Ke(t) \tag{56}$$

with $K = \frac{1}{r}B^T P$ where P is a positive definite symmetric matrix which is obtained from the solution of the Riccati equation

$$A^T P + PA + Q - P(\tfrac{2}{r}BB^T - \tfrac{1}{\rho^2}LL^T)P = 0 \tag{57}$$

where Q is also a positive semi-definite symmetric matrix. The worst case disturbance is given by $\tilde{d}(t) = \frac{1}{\rho^2}L^T Pe(t)$ The computation of the worst-case disturbance that this controller can sustain, comes from superposition of Bellman's optimality principle when considering that the motor is affected by two separate inputs, that is the control input u and the cumulative disturbance input $\tilde{d}$. From the previous relation about the worst case disturbance it can be seen that the smallest value of the attenuation coefficient ρ that results into an admissible solution for the method's algebraic Riccati equation, is the one that provides the control loop with maximum robustness. The diagram of the considered control loop is depicted in Fig. 3.

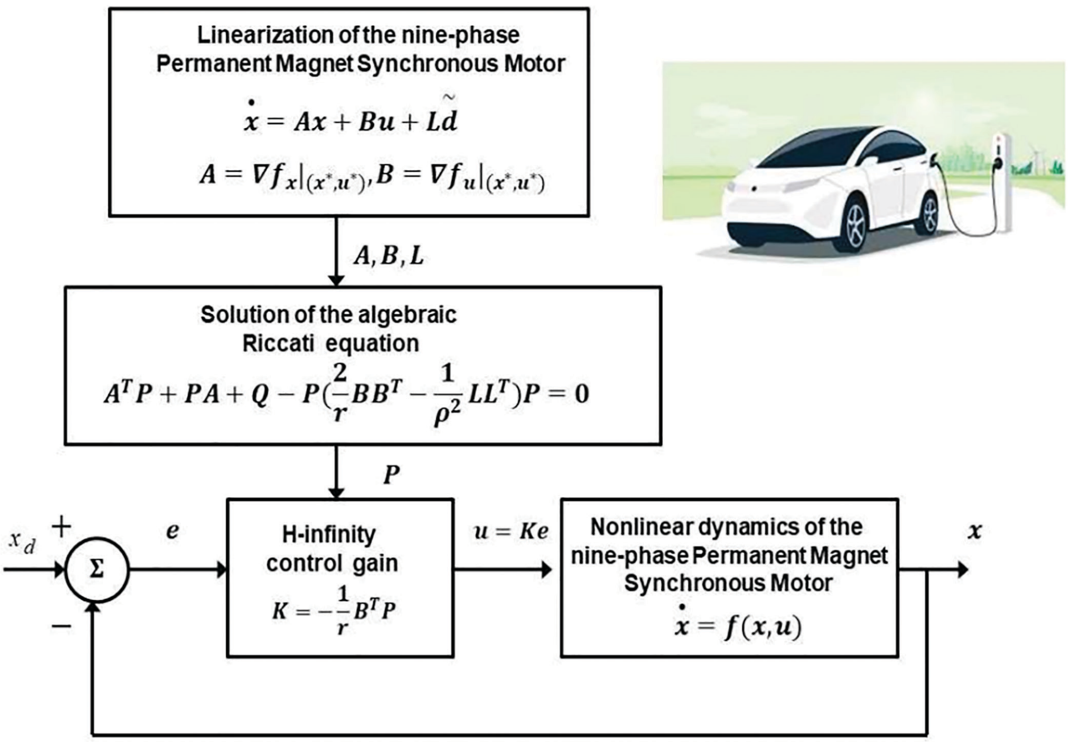

Fig. 3. Diagram of the Nonlinear Optimal Control loop for a 9-phase PMSM.

6. Lyapunov stability analysis

6.1 Stability proof

Through Lyapunov stability analysis it will be shown that the proposed nonlinear control scheme assures H_∞ tracking performance for the 9-phase PMSM, and that in case of bounded disturbance terms asymptotic convergence to the reference setpoints is achieved. The tracking error dynamics for the 9-phase PMSM is written in the form (Rigatos, 2016)

$$\dot{e} = Ae + Bu + L\tilde{d} \tag{58}$$

where in the 9-phase PMSM's case $L \in R^{8\times 8}$ is the disturbance inputs gain matrix. Variable $\tilde{d}$ denotes model uncertainties and external disturbances of the motor's model. The following Lyapunov equation is considered

$$V = \frac{1}{2}e^T Pe \tag{59}$$

where $e = x - x_d$ is the tracking error. By differentiating with respect to time one obtains

$$\begin{gathered}\dot{V} = \frac{1}{2}\dot{e}^T Pe + \frac{1}{2}e^T P\dot{e} \Rightarrow \\ \dot{V} = \frac{1}{2}[Ae + Bu + L\tilde{d}]^T Pe + \frac{1}{2}e^T P[Ae + Bu + L\tilde{d}] \Rightarrow\end{gathered} \tag{60}$$

$$\begin{aligned}\dot{V} = &\frac{1}{2}[e^T A^T + u^T B^T + \tilde{d}^T L^T]Pe + \\ &+\frac{1}{2}e^T P[Ae + Bu + L\tilde{d}] \Rightarrow\end{aligned} \tag{61}$$

$$\begin{aligned}\dot{V} = &\frac{1}{2}e^T A^T Pe + \frac{1}{2}u^T B^T Pe + \frac{1}{2}\tilde{d}^T L^T Pe + \\ &\frac{1}{2}e^T PAe + \frac{1}{2}e^T PBu + \frac{1}{2}e^T PL\tilde{d}\end{aligned} \tag{62}$$

The previous equation is rewritten as

$$\begin{aligned}\dot{V} = &\frac{1}{2}e^T (A^T P + PA)e + (\frac{1}{2}u^T B^T Pe + \frac{1}{2}e^T PBu) + \\ &+(\frac{1}{2}\tilde{d}^T L^T Pe + \frac{1}{2}e^T PL\tilde{d})\end{aligned} \tag{63}$$

Assumption: For given positive definite matrix Q and coefficients r and ρ there exists a positive definite matrix P, which is the solution of the following matrix equation

$$A^T P + PA = -Q + P(\frac{2}{r}BB^T - \frac{1}{\rho^2}LL^T)P \tag{64}$$

Moreover, the following feedback control law is applied to the system

$$u = -\frac{1}{r}B^T Pe \tag{65}$$

By substituting Eq. (64) and Eq. (65) one obtains

$$\begin{aligned}\dot{V} = &\frac{1}{2}e^T [-Q + P(\frac{2}{r}BB^T - \frac{1}{\rho^2}LL^T)P]e + \\ &+e^T PB(-\frac{1}{r}B^T Pe) + e^T PL\tilde{d} \Rightarrow\end{aligned} \tag{66}$$

$$\begin{aligned}\dot{V} = &-\frac{1}{2}e^T Qe + (\frac{1}{r}e^T PBB^T Pe - \frac{1}{2\rho^2}e^T PLL^T Pe) \\ &-\frac{1}{r}e^T PBB^T Pe + e^T PL\tilde{d}\end{aligned} \tag{67}$$

which after intermediate operations gives

$$\dot{V} = -\frac{1}{2}e^TQe - \frac{1}{2\rho^2}e^TPLL^TPe + e^TPL\tilde{d} \tag{68}$$

or, equivalently

$$\begin{aligned}\dot{V} = -\frac{1}{2}e^TQe - \frac{1}{2\rho^2}e^TPLL^TPe+ \\ +\frac{1}{2}e^TPL\tilde{d} + \frac{1}{2}\tilde{d}^TL^TPe\end{aligned} \tag{69}$$

Lemma: The following inequality holds (Rigatos, 2016)

$$\frac{1}{2}e^TL\tilde{d} + \frac{1}{2}\tilde{d}L^TPe - \frac{1}{2\rho^2}e^TPLL^TPe \leq \frac{1}{2}\rho^2\tilde{d}^T\tilde{d} \tag{70}$$

Proof : The binomial $(\rho\alpha - \frac{1}{\rho}b)^2$ is considered. Expanding the left part of the above inequality one gets

$$\begin{aligned}\rho^2a^2 + \frac{1}{\rho^2}b^2 - 2ab \geq 0 \Rightarrow \frac{1}{2}\rho^2a^2 + \frac{1}{2\rho^2}b^2 - ab \geq 0 \Rightarrow \\ ab - \frac{1}{2\rho^2}b^2 \leq \frac{1}{2}\rho^2a^2 \Rightarrow \frac{1}{2}ab + \frac{1}{2}ab - \frac{1}{2\rho^2}b^2 \leq \frac{1}{2}\rho^2a^2\end{aligned} \tag{71}$$

The following substitutions are carried out: $a = \tilde{d}$ and $b = e^TPL$ and the previous relation becomes

$$\frac{1}{2}\tilde{d}^TL^TPe + \frac{1}{2}e^TPL\tilde{d} - \frac{1}{2\rho^2}e^TPLL^TPe \leq \frac{1}{2}\rho^2\tilde{d}^T\tilde{d} \tag{72}$$

Eq. (72) is substituted in Eq. (69) and the inequality is enforced, thus giving (Rigatos, 2016)

$$\dot{V} \leq -\frac{1}{2}e^TQe + \frac{1}{2}\rho^2\tilde{d}^T\tilde{d} \tag{73}$$

Eq. (73) shows that the H_∞ tracking performance criterion is satisfied. The integration of $\dot{V}$ from 0 to T gives

$$\begin{aligned}\int_0^T\dot{V}(t)dt \leq -\frac{1}{2}\int_0^T||e||_Q^2dt + \frac{1}{2}\rho^2\int_0^T||\tilde{d}||^2dt \Rightarrow \\ 2V(T) + \int_0^T||e||_Q^2dt \leq 2V(0) + \rho^2\int_0^T||\tilde{d}||^2dt\end{aligned} \tag{74}$$

Moreover, if there exists a positive constant $M_d > 0$ such that

$$\int_0^\infty ||\tilde{d}||^2dt \leq M_d \tag{75}$$

then one gets

$$\int_0^\infty ||e||_Q^2dt \leq 2V(0) + \rho^2M_d \tag{76}$$

Thus, the integral $\int_0^\infty ||e||_Q^2dt$ is bounded. Moreover, $V(T)$ is bounded and from the definition of the Lyapunov function V in Eq. (59) it becomes clear that $e(t)$ will be also bounded since $e(t) \in \Omega_e = \{e|e^TPe \leq 2V(0) + \rho^2M_d\}$. According to the above and with the use of Barbalat's Lemma one obtains $lim_{t\to\infty}e(t) = 0$.

After following the stages of the stability proof one arrives at Eq. (73) which shows that the H-infinity tracking performance criterion holds. By selecting the attenuation coefficient ρ to be sufficiently small and in particular to satisfy $\rho^2 < ||e||_Q^2/||\tilde{d}||^2$ one has that the first derivative of the Lyapunov function is upper bounded by 0. This condition holds at each sampling instance and consequently global stability for the control loop can be concluded.

6.2 Robust state estimation with the use of the H_∞ Kalman Filter

The control loop has to be implemented with the use of information provided by a small number of sensors and by processing only a small number of state variables. Actually, one can implement feedback control by measuring only the stator currents. To reconstruct the missing information about the state vector of the 9-phase PMSM it is proposed to use a filtering scheme and based on it to apply state estimation-based control (Rigatos, 2016). By denoting as $A(k),\ B(k)$ and $C(k)$ the discrete-time equivalents of matrices *A*, *B* and *C* of the linearized state-space model of the system, the recursion of the H_∞ Kalman Filter, for the model of the 9-phase PMSM can be formulated in terms of a *measurement update* and a *time update* part

Measurement update:

$$\begin{array}{l} D(k) = [I - \theta W(k)P^-(k) + C^T(k)R(k)^{-1}C(k)P^-(k)]^{-1} \\ K(k) = P^-(k)D(k)C^T(k)R(k)^{-1} \\ \hat{x}(k) = \hat{x}^-(k) + K(k)[y(k) - C\hat{x}^-(k)] \end{array} \tag{77}$$

Time update:

$$\begin{array}{l} \hat{x}^-(k+1) = A(k)x(k) + B(k)u(k) \\ P^-(k+1) = A(k)P^-(k)D(k)A^T(k) + Q(k) \end{array} \tag{78}$$

where it is assumed that parameter θ is sufficiently small to assure that the covariance matrix $P^-(k)^{-1} - \theta W(k) + C^T(k)R(k)^{-1}C(k)$ will be positive definite. When $\theta = 0$ the H_∞ Kalman Filter becomes equivalent to the standard Kalman Filter. One can measure only a part of the state vector of the nine-phase PMSM, and can estimate through filtering the rest of the state vector elements. For instance, one can measure the rotor's turn angle $x_1 = \theta$, and the stator currents $x_3,\ x_4,\ x_5,\ x_6,\ x_7,\ x_8$ and can estimate through filtering the rotor's turn speed x_2.

7. Simulation tests

The previously proven global stability properties of the nine-phase PMSM are further confirmed through simulation experiments. To implement the nonlinear optimal control method, the algebraic Riccati equation of Eq. (64) had to be repetitively solved, at each time-step of the control algorithm using Matlab's $aresolv()$ function. Indicative values about the parameters of the 9-phase PMSM are as follows: number of phases $P_m = 4$, moment of inertia of the rotor $J = 1.4kg{\cdot}m^2$, damping coefficient $b_m = 0.01$, magnetic flux due to permanent magnets $\Psi_m = 3.1Wb$, resistance of the stator $R_s = 0.3Ohm$, d-axis component of self-inductance $L_d = 85mH$, q-axis component of self-inductance $L_q = 84mH$, d-axis component of mutual-inductance $M_d = 13mH$, q-axis component of mutual-inductance $M_q = 12mH$, mass of the load $m_L = 1.2kg$, length of the rod carrying the load $l_L = 1.0m$, gravity's acceleration $g = 10m/sec^2$. The control method is sufficiently robust to model uncertainty and parametric imprecision and performs well even when the controller uses distorted values of the parameters of the 9-phase PMSM.

The obtained results are depicted in Fig. 4 to Fig. 7. The sampling period was $T_s = 0.01\mathrm{sec}$. The method is computationally efficient since the time needed to solve the Riccati equation in a PC with an Intel i7 processor at 2.8HGz is much shorter than the sampling interval. As it can be noticed from the simulation experiments the method achieves fast and accurate tracking of setpoints by all state variables of the 9-phase PMSM while the variations of the control inputs remain moderate. The parameters which affect the transient performance of the control scheme are coefficients $r,\ \rho$ and Q in the Riccati equation.

For relatively small values of *r* the tracking error of the state variables is eliminated, while for relatively large values of Q fast convergence to the reference values is achieved. Moreover, the smallest value of ρ for which a valid solution of the method's Riccati equation is obtained in the form of a positive definite and symmetric matrix *P* is the one that provides the control loop with maximum robustness.

The setpoints for the state variable of the 9-phase PMSM have been selected as follows: for state variable x_1 (that is the turn angle of the 9-phase PMSM) each setpoint is a sum of sinusoidal signals, while for state variable x_2

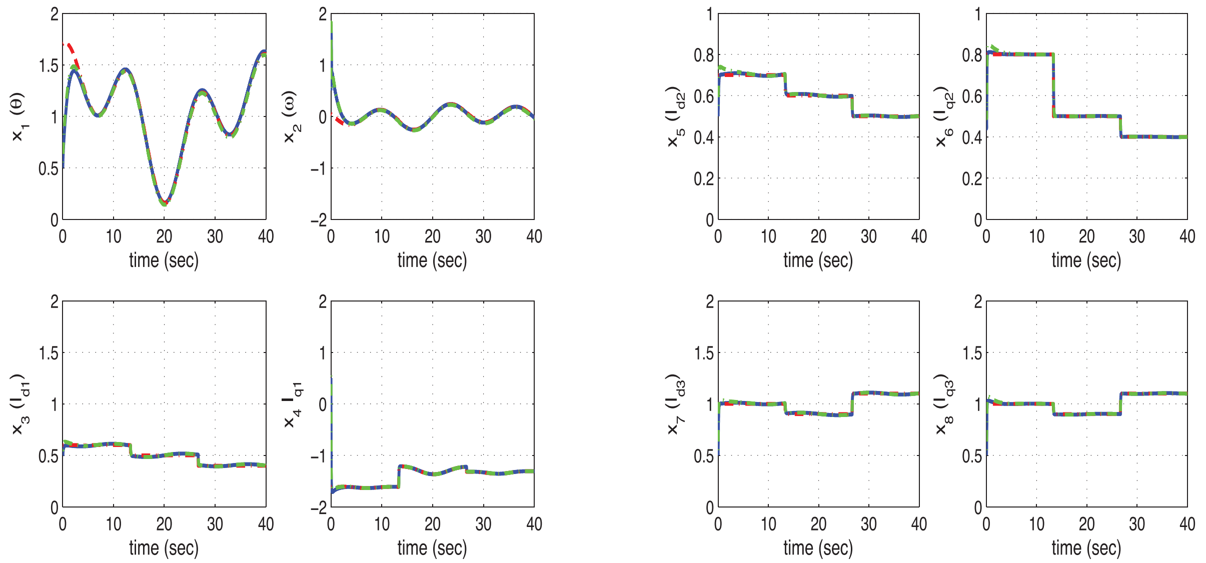

(a) (b)

Fig. 4. Tracking of setpoint 1 by the nine-phase PMSM (a) convergence of state variables x_1 to x_4 to their reference setpoints (red line: setpoint, blue line: real value, green line: estimated value), (b) convergence of state variables x_5 to x_8 to their reference setpoints (red line: setpoint, blue line: real value, green line: estimated value).

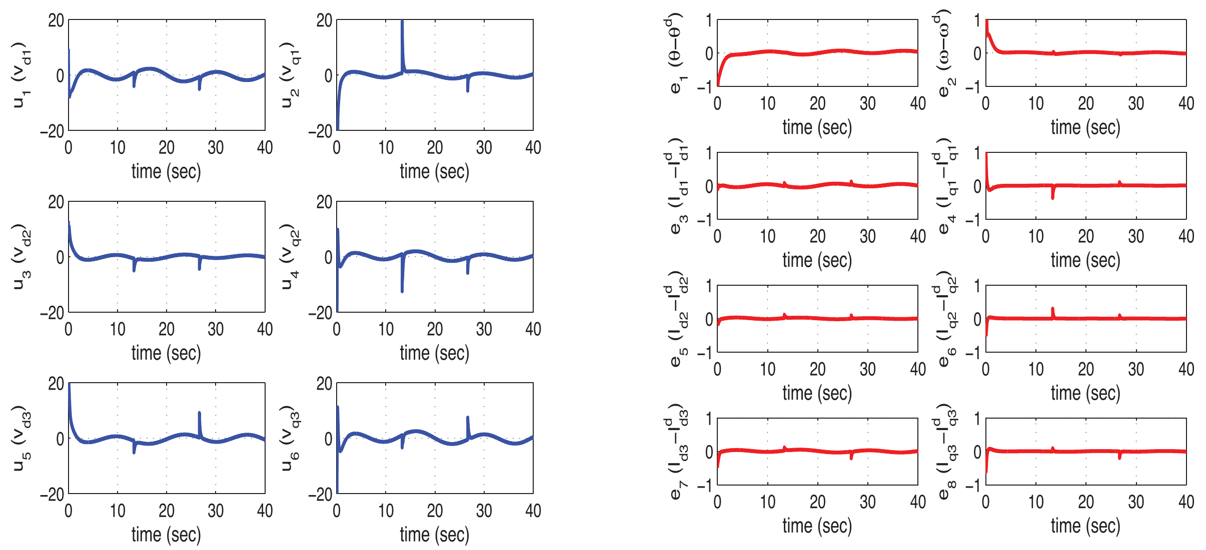

(a) (b)

Fig. 5. Tracking of setpoint 1 by the nine-phase PMSM (a) control inputs u_1 to u_6, (b) convergence to zero of the tracking error for the indicative state variables of the nine-phase PMSM.

(which is the angular speed of the motor) the setpoint is the time-derivative of the setpoint of x_1. Convergence of x_1 and x_2 to such a type of sinusoidal setpoints demonstrates the capability of the proposed nonlinear optimal control method for precise positioning of the rotor and for reliable functioning of the multi-phase motor under variable angular speed. (ii) for state variables x_3 to x_8 (which are the currents of the phases of the 9-phase PMSM), the associated setpoints exhibit stepwise changes. Despite these abrupt changes it can be noticed that the nonlinear optimal control method achieves again fast convergence of the current state variables to the targeted reference

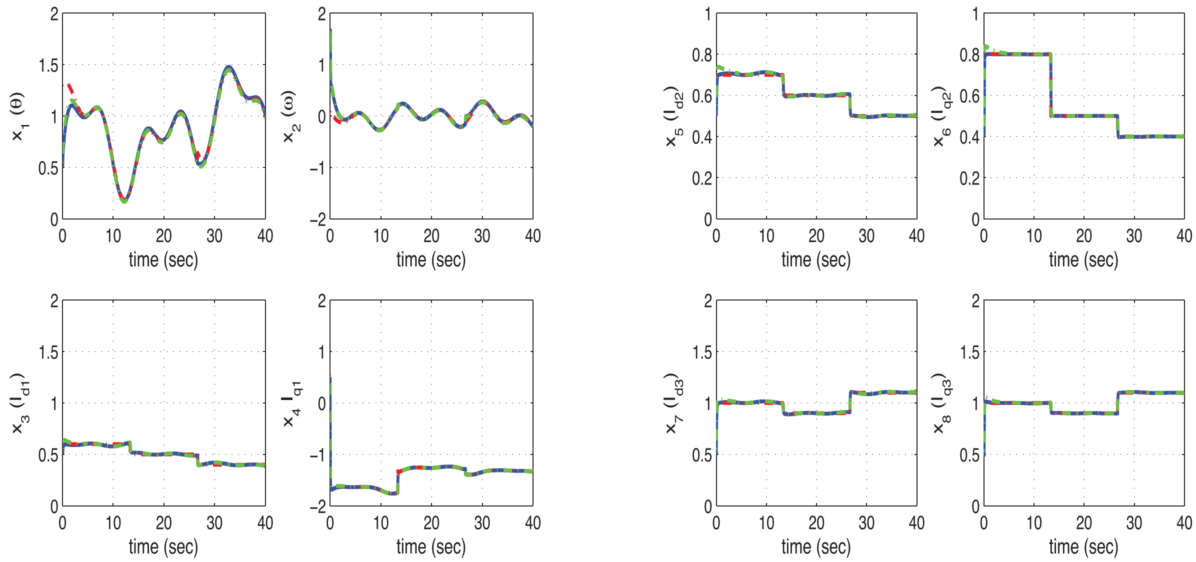

(a) (b)

Fig. 6. Tracking of setpoint 2 by the nine-phase PMSM (a) convergence of state variables x_1 to x_4 to their reference setpoints (red line: setpoint, blue line: real value, green line: estimated value), (b) convergence of state variables x_5 to x_8 to their reference setpoints (red line: setpoint, blue line: real value, green line: estimated value).

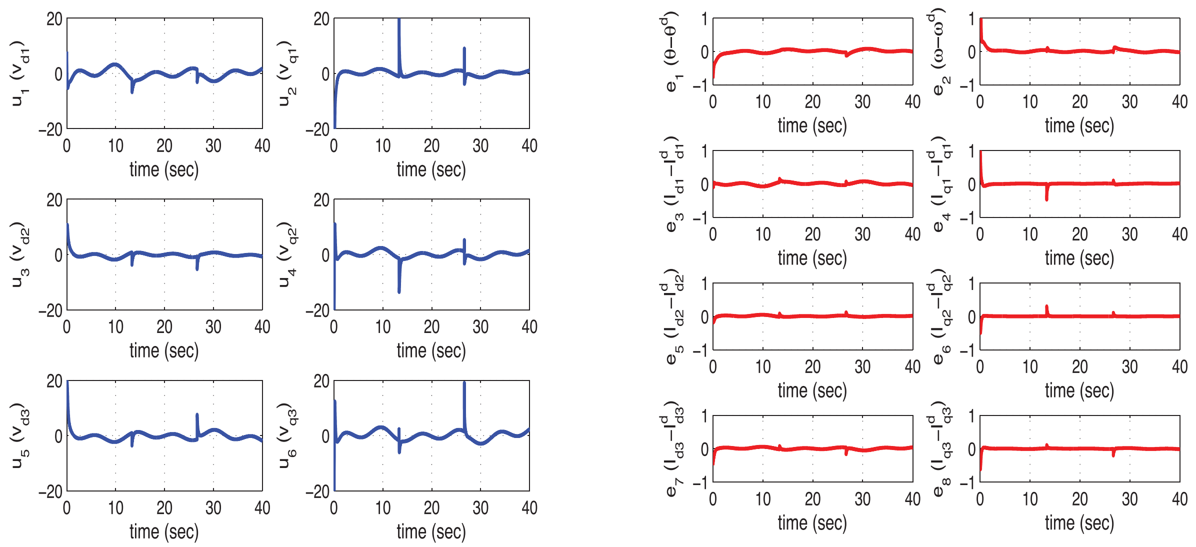

(a) (b)

Fig. 7. Tracking of setpoint 2 by the nine-phase PMSM (a) control inputs u_1 to u_6, (b) convergence to zero of the tracking error for the indicative state variables of the nine-phase PMSM.

values. Tracking of time-variable setpoints is also an evidence about the global stability properties of the control method.

Comparing to other nonlinear approaches that one could have considered for the dynamic model of the 9-phase PMSM the article's nonlinear optimal control method exhibits specific advantages. These are outlined in the following: (i) Compared to global linearization-based techniques such as Lie algebra-based control and flatness-based control through transformation into canonical forms and eigenvalues assignment the proposed nonlinear optimal control method does not need complicated state-space model transformations with the definition of new state variables (diffeomorphisms). The optimal control is applied directly on the initial nonlinear state space model of the system without involving inverse transformations that may come against singularity issues, (ii) compared to popular approaches for treating the optimal control problem in industry, such as Nonlinear Model Predictive Control (NMPC) the proposed nonlinear optimal control method is of proven global stability and its convergence to optimum does not depend on parameter values selection and on initialization (multiple shooting methods), (iii) compared to sliding-mode control the nonlinear optimal control method does not need the controlled system to be found or to be transformed into a specific state-space form. For instance it is known that unless the system is in the input-output linearized form (canonical form) there is no systematic manner for defining sliding surfaces and for computing the sliding-mode control inputs, (iv) compared to backstepping control the nonlinear optimal control method does not need the controlled system to be found or to be transformed into a specific state-space form. For instance in backstepping control unless the system is found in the triangular (strict feedback) form there is no systematic manner to compute the stabilizing feedback control inputs, (v) unlike multiple local-models feedback control the proposed nonlinear optimal control approach does not induce an excessive computational load. It does not need linearization around multiple arbitrarily chosen operating points and does not require the solution of multiple Riccati equations or LMIs (vi) compared to PID-type control, the nonlinear optimal control method does not follow a heuristics-based selection of controller parameters and ensures global stability in changes of operating points and under variable operating conditions.

It is also of worth to point out that in synchronous and asynchronous electric machines the control problem is usually solved through a forward transformation of voltage, current and magnetic flux variables in a rotating reference frame, while to obtain representation of these variables in the phases' frame an inverse transformation is needed. For instance, in the case of three-phase machines, after using Clarke's / Park's transformation one moves from the abc frame with sinusoidal voltage and current waveforms to the dq0 frame with amplitude voltage and current representation. Inverting the transformation allows to reconstruct the sinusoidal voltage and current signals of the phases of the electric machine. In the case of the article's 9-phase machine one uses a 3-phase Clarke's / Park's transformation and its inverse for the voltage and current variables of each one of the three 3-phase frames $a_1b_1c_1$, $a_2b_2c_2$ and $a_3b_3c_3$ which constitute the electric dynamics of the 9-phase motor. Thus, using the inverse of the Clarke's / Park's transformation matrix of Eq. (34) (i) the variation of the phase currents of the 1st 3-phase frame

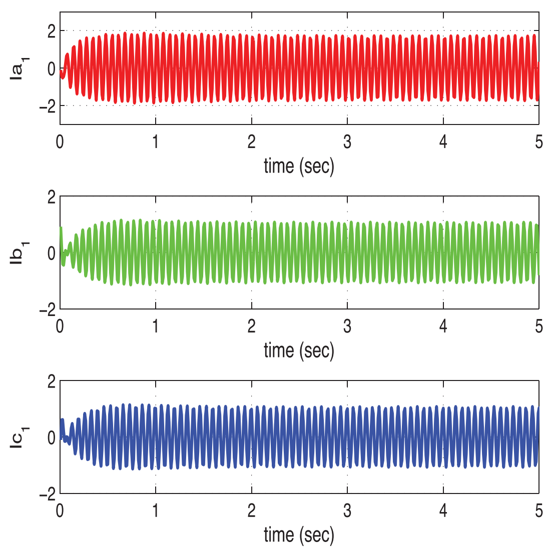

(a)

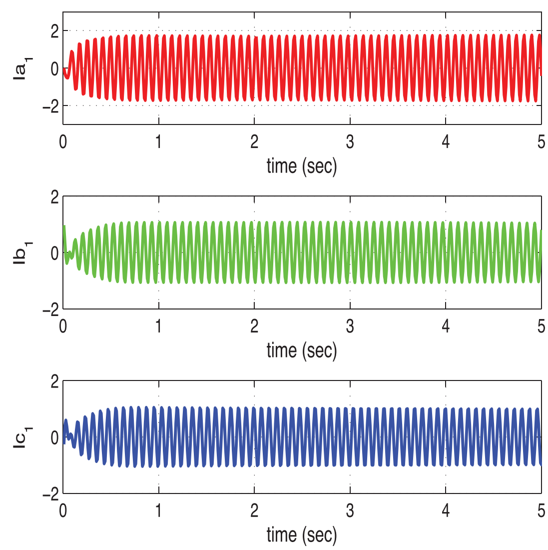

(b)

Fig. 8. Variation of the phase currents of the 1st 3-phase frame of the 9-phase PMSM: (a) when tracking setpoint 1, (b) when tracking setpoint 2.

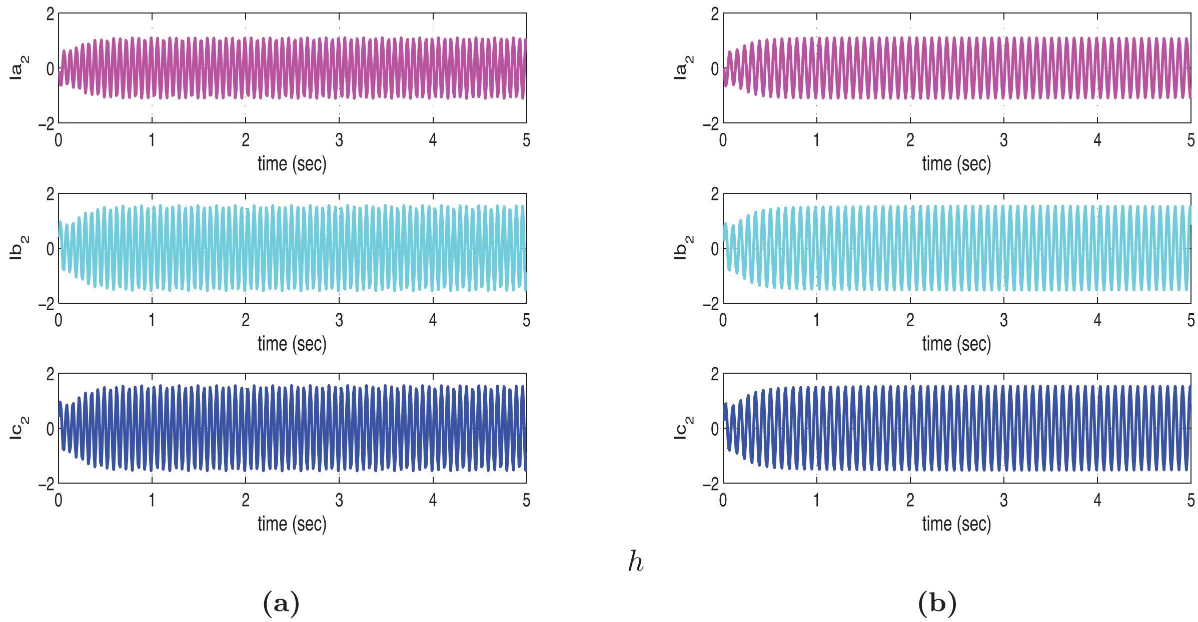

Fig. 9. Variation of the phase currents of the 2nd 3-phase frame of the 9-phase PMSM: (a) when tracking setpoint 1, (b) when tracking setpoint 2.

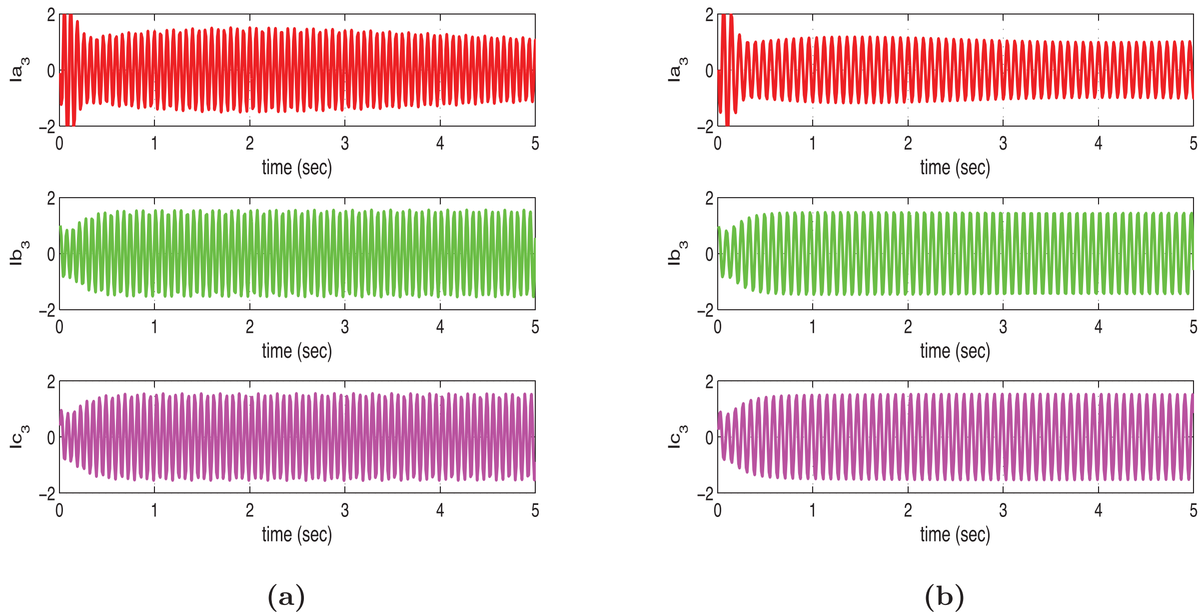

Fig. 10. Variation of the phase currents of the 3rd 3-phase frame of the 9-phase PMSM: (a) when tracking setpoint 1, (b) when tracking setpoint 2.

of the 9-phase PMSM $a_1b_1c_1$ are shown in the diagrams of Fig. 8 , (ii) the variation of the phase currents of the 2nd 3-phase frame of the 9-phase PMSM $a_2b_2c_2$ are shown in the diagrams of Fig. 9, (iii) the variation of the phase currents of the 3rd 3-phase frame of the 9-phase PMSM $a_3b_3c_3$ are shown in the diagrams of Fig. 10.

To elaborate on the previous diagrams and on the fine tracking performance and the global stability properties of the nonlinear optimal control method for the 9-phase PMSM, the following Tables are also given: (i) Table 1 providing data about the accuracy of tracking of setpoints by the state variables of the 9-phase PMSM under an

No test	$RMSE_{x_1}$	$RMSE_{x_2}$	$RMSE_{x_3}$	$RMSE_{x_4}$	$RMSE_{x_5}$	$RMSE_{x_6}$	$RMSE_{x_7}$	$RMSE_{x_8}$
test1	0.4861	0.0615	0.1311	0.0514	0.0279	0.0210	0.0776	0.0464
test2	0.8440	0.0637	0.0745	0.0297	0.0405	0.0142	0.1006	0.0342

Table 1. Tracking RMSE for the 9-phase in the disturbance-free case $\times\ 10^{-3}$

No test	$RMSE_{\hat{x}_1}$	$RMSE_{\hat{x}_2}$	$RMSE_{\hat{x}_3}$	$RMSE_{\hat{x}_4}$	$RMSE_{\hat{x}_5}$	$RMSE_{\hat{x}_6}$	$RMSE_{\hat{x}_7}$	$RMSE_{\hat{x}_8}$
test1	0.3639	0.6976	0.0001	0.0001	0.0001	0.0001	0.0001	0.0001
test2	0.4373	0.7684	0.0001	0.0001	0.0001	0.0001	0.0001	0.0001

Table 2. Estimation RMSE for the H-infinity Kalman Filter $\times\ 10^{-3}$

No test	$T_s\ x_1$	$T_s\ x_2$	$T_s\ x_3$	$T_s\ x_4$	$T_s\ x_5$	$T_s\ x_6$	$T_s\ x_7$	$T_s\ x_8$
test1	3.5	4.0	0.2	0.2	0.2	0.2	0.2	0.2
test2	3.5	3.0	0.2	0.2	0.2	0.2	0.2	0.2

Table 3. Convergence times (sec) for the 9-phase PMSM

exact dynamic model, (ii) Table 2 providing data about the accuracy of state estimation that is achieved by the H-infinity Kalman Filter, (iii) Table 3 providing data about the speed of convergence of the state variables of the 9-phase PMSM to the targeted setpoints.

8. Conclusions

Nine-phase permanent magnet synchronous motors exhibit specific advantages when compared to three-phase synchronous or asynchronous motors. They can produce higher power and torque while keeping moderate the values of currents and voltages at their phases, they are less prone to a total failure and they can remain functional under harsh operating conditions. Based on these merits, nine-phase PMSMs are also a reliable solution for the traction problem of heavy-duty vehicles. Due to the nonlinear and multivariable structure of the dynamic model of nine-phase PMSMs the solution of the associated feedback control problem is a nontrivial task. In this article a novel nonlinear optimal (H-infinity) controller is developed for a nine-phase PMSM. To this end, the dynamic model of the nine-phase PMSM undergoes approximate linearization with the use of first-order Taylor-series expansion and through the computation of the associated Jacobian matrices. The linearization takes place at each sampling instance around a temporary operating point which is defined by the present value of the system's state vector and by the last sampled value of the control inputs vector.

The model imprecision which is due to the truncation of higher-order terms from the Taylor series is viewed as a perturbation which is asymptotically compensated by the robustness of the control method. The nonlinear optimal controller represents a differential game which takes place between the control inputs and the modelling errors or the exogenous perturbations that affect the system. For the approximately linearized model of the nine-phase PMSM an H-infinity optimal feedback controller is designed. To select the feedback gains of the controller an algebraic Riccati equation is solved at each sampling instant. The global stability properties of the control scheme are proven through Lyapunov analysis. By demonstrating that the H-infinity tracking performance criterion holds the robustness of the control method to model uncertainty and external perturbations has been confirmed. Moreover, under moderate conditions, it has been proven that the control method is globally asymptotically stable. The nonlinear optimal control approach for nine-phase PMSMs retains the advantages of typical linear optimal control, that is fast and accurate tracking of setpoints under moderate variations of the control inputs.

Acknowledgements

(a) Gerasimos Rigatos has been partially supported by Grant Ref. 301022 “Nonlinear optimal and flatness-based control methods for complex dynamical systems” of the Unit of Industrial Automation, Industrial Systems Institute, Greece (b) Pierluigi Siano and Mohammed AL-Numay acknowledge financial support from the Researchers Supporting Project Number (RSP2023R150), King Saud University, Riyadh, Saudi Arabia.

References

Basseville M. and Nikiforov I. (1993). Detection of abrupt changes: Theory and Applications. Prentice-Hall, New Jersey, USA.

Cheng M., Yu F., Chou K.T and Hua W. (2016). Dynamic performance evaluation of a nine-phase fluxswitching permanent magnet motor drive with model predictive control. IEEE Transactions on Industrial Electronics. 63(7): 4539-4549.

Garcia-Entrambosaguas P., Zoric I., Gonzalez-Prieto I., Duran M.J. and Lewi E. (2019). Direct torque and predictive control strategies in nine-phase electric drives using virtual voltage vectors. IEEE Transactions on Power Electronics. 34(12): 12106-12119.

Jung E., You H., Sul S.K., Choi H.S. and Choi Y.Y. (2012). A nine-phase permanent magnet motor drive system for an ultrahigh-speed elevator. IEEE Transactions on Industry Applications. 48(3): 987-996.

Kozovsky M., Blaha P. and Vaclaveck P. (2016). Verification of nine-phase PMSM model in d-q coordinats with mutual couplings. IEEE ICCSCE 2016, IEEE 7th Intl. Conference on Control Systems, Computing and Engineering, Penang, Malaysia.

Kozovsky M. and Blaha P. (2017). Simulink generated control algorithm for nine-phase PMS motor. IEEE ICCSCE 2017, IEEE 7th Intl. Conference on Control Systems, Computing and Engineering, Penang, Malaysia.

Liu X., Zhang X. and Zheng X. (2020). Sensorless fault-tolerant control of a nine-phase Permanent Magnet Synchronous Motor under one-phase open-circuited fault. IEEE ICEMS 2023, IEEE 25th Intl. Conference on Electrical Machines and Drives, Chiang May, Thailand.

Mohamadian S. and Cecati C. (2021). Modeling, harmonic compensation and current sharing between winding sets of asymmetric nine-phase PMSM. IEEE IECON 2021, IEEE 47th Annual Conference of the IEEE Industrial Electronics Society, Toronto, Canada.

Mohamadian S., Tedeschini S. and Cecati C. (2023). Modelling and fault-toleerant control of triple three-phase PMSM under open-phase fault with mimimum stator power losses. IEEE IECON 2022, IEEE 48th Annual Conference of the Industrial Electronics Society, Brussels, Belgium.

Prieto-Araujo E., Junyent-Ferr´e A., Lav`ernia-Ferrer D. and Gomis-Bellmunt O. (2015). Decentralized control of a nine-phase Permanent Magnet generator for offshore wind-turbines. IEEE Transactions on Energy Conversion. 30(3): 1103-1112.

Rigatos G. and Tzafestas S. (2007). Extended Kalman Filtering for Fuzzy Modelling and Multi-Sensor Fusion, Mathematical and Computer Modelling of Dynamical Systems. Taylor & Francis, 13: 251-266, 2007.

Rigatos G. and Zhang Q. (2009). Fuzzy model validation using the local statistical approach. Fuzzy Sets and Systems. Elsevier, 60(7): 882-904.

Rigatos G. (2015). Nonlinear control and filtering using differential flatnesss theory approaches: Applications to electromechanical systems. Springer, Cham, Switzerland.

Rigatos G. (2016). Intelligent Renewable Energy Systems: Modelling and Control. Springer, Cham, Switzerland.

Rigatos G. and Karapanou E. (2020). Advances in applied nonlinear optimal control. Cambridge Scholars Publishing, Newcastle, UK.

Rigatos G., Abbaszadeh M. and Hamida M.A. (2023). Nonlinear control, estimation and fault diagnossis for electric power generation, traction and propulsion systems. monograph in press, 2023.

Rubins S., Dordevic O., Armando E., Bojoi R. and Levi E. (2020). A novel matrix transformation for decoupled control of modular multi-phase PMSM drives. IEEE Transactions on Power Electronics. 36(7): 8088-8101.

Stiscia O., Slunjski M., Levi E. and Cavagnini A. (2019). Sensorless control of a nine-phase surface mounted Permanent Magnet Synchronous Machine with highly non-sinusoidal back-EMF. IEEE IECON 2019, IEEE 45th Annual Conference of the Industrial Electronics Society, Lisbon, Portugal.

Slunjski M., Sascia O., Jones M. and Levi E. (2021). General torque enhancement approach for a ninephase surface PMSM with built-in fault tolerance. IEEE Transactions on Industrial Electronics. 68(8): 6412-6423.

Slunjski M., Jones M. and Levi E. (2019). Control of a symmetrical nine-phase PMSM with highly nonsinusoidal back-electromotive force using third harmonic current injection. IEEE IECON 2019, IEEE 45th Annual Conferenc of the Industrial Electronics Society, Lisbon, Portugal.

Tong M., Chen Y., Yang T. and Ilkhami M. (2022). Comparison of three speed-loop designs for a highspeed nine-phase permanent magnet synchronous machine in more electric aircraft. IEEE IECON 2022, IEEE 48th Annual Conference of the Industrial Electronics Society, Brussels, Belgium.

Toussaint G.J., Basar T. and Bullo F. (2000). $H\infty$ optimal tracking control techniques for nonlinear underactuated systems. Proc. IEEE CDC 2000, 39th IEEE Conference on Decision and Control, Sydney Australia.

Wang B., Xu Y., Wang R. and Chang M. (2023). Advanced fault tolerant 3×3 phase PM drive with concentric winding for EV application. IEEE Transaction on Transportation Electrification. 1-11.

Wang B., Zhu C., Xu Y., Wang J., Chen M. and Hua W. (2023). Comparative-study on fault tolerant triple-phase PM machine drive with five modular windings. IEEE Transactions on Industrial Electronics. 70(10): 9720-9730.

Wang H., Zheng X., Yuan X. and Wu X. (2022). Low-complexity model predictive control for a nine-phase open-end winding PMSM with dead-time compensation. IEEE Transactions on Power Electronics. 37(8): 8895-8908.

Wang H., Wu X., Zheng X. and Yuan X. (2023). Model predictive current control of nine-phase openend winding PMSM with an online virtual vector synthesis strategy. IEEE Transactions on Industrial Electronics. 78(3):2199-2208.

Wang S., Imai K. and Doki S. (2023). A Novel Decoupling Control Scheme for Non-Salient Multi-ThreePhase Synchronous Machines Based on Multi-Stator Model. IEEE Transactions on Industry Applications. 58(1): 886-896.

Wang H., Wu X., Zheng X. and Yuan X. (2022). Virtual Voltage Vector-based model predictive control for a nine-phase open-end winding PMSM with a common DC bus. IEEE Transactions on Industrial Electronics. 69(5): 5386-5397.

Wang Z., Wu X. and Wang H. (2022). Sensorless control strategy of nine-phase PMSM based on piecewise combination of open-loop and sliding-mode observer. IEEE CIEEC 2022, IEEE 2022 5th Itl. Electrical and Energy Conference, Nangjing, China.

Zhai Z., Li C., Li M. and Zhang X. (2020). Vector control of nine-phase permanent magnet synchronous motor under symmetrical fault condition for derating operation. IEEE ICEMS 2020, IEEE 2020 23rd Intl. Conference on Electrical Machines and Systems, Hamamatsu Japan.